The effect of differential compaction on shelf-edge trajectories

Part I: Decompaction of clinoform successions
Part II: Implications to predictive capacity

1st supervisor: Professor Christopher Aiden-Lee Jackson (Imperial College London)
2nd supervisor: Assistant-Professor João Trabucho-Alexandre (Utrecht University)
Student: Daan Beelen

October 2017

Part I: Decompaction of clinoform successions

Part II: Implications to predictive capacity

APPENDIX

The effect of differential compaction on shelf-edge trajectories

Part I: Decompaction of clinoform successions

ABSTRACT

Clinoforms are sigmoidal strata that prograde toward the deep part of a basin. Their geometry allows us to define shelf-edge trajectories, which are then used to infer temporal and spatial variations in sediment transfer, relative sea-level change and paleobathymetric configurations. Trajectory analysis is typically conducted on deeply buried successions, in which the primary stratigraphic architecture is modified by sediment compaction. Furthermore, the impact of dip-oriented lithological heterogeneity within clinothems during compaction is not considered. Here, we present a new approach to decompaction of clinothems that accounts explicitly for the down-dip variation in their lithology. This approach reveals that greater, or preferential, compaction of fine-grained foresets and bottomsets results in a basinward rotation of trajectories. In some cases, shelf-edge trajectories can change from rising, normal regressive trajectories to apparently falling, forced regressive trajectories, leading to erroneous interpretations for the timing and volume of sediment transfer. Also, preferential compaction counter-intuitively steepens and vertically extends rather than compresses clinothems after burial. This opposes the results of decompaction methods that do not account for basinward variations in lithology and affects interpretations of paleobatymetry and slope processes, thus implying a lithologically controlled component onto the traditional understanding of trajectory analyses, sequence stratigraphy and clinoform geometry analysis.

Clinoform trajectories and sequence stratigraphy

In basin analyses and petroleum exploration it is of great relevance to classify episodes in the deposition of basin sediments by means of their stratal geometries. This is because seismic and well data provide no or very limited insights into lithological composition and depositional history. Sequence stratigraphy and clinoform trajectory analysis are widely used concepts for translating stratal geometries into a more useful four-dimensional interpretation of the subsurface that includes potentially vital information on the basin's depositional history and distribution of lithologies. These concepts rely on the geometries of strata located at the transition from continents to basins known as clinoforms. Clinoforms or, clinoformal strata, are usually sigmoidal in shape and can be deposited vertically; known as aggradation (upward) or degradation (downward) and horizontally; towards the basin (progradation) or from the basin (retrogradation). The clinoform trajectory is a line drawn through a series of points on clinoforms known as rollover points, starting from the oldest, moving through consecutively younger strata (Helland-Hansen and Gjelberg, 1994). It represents the transit of the clinoform rollover points through space in a cross-depositional dip-section of a clinoform succession. Trajectory gradients and orientations therefore indicate the direction of stratal stacking, meaning; the proportion of aggradation/degradation to progradation/retrogradation and thereby reflect changes in relative sea-level and episodes of basin evolution which can then be classified into genetically linked deposits (e.g. systems tracts) that are associated with certain lithological and genetic characteristics.

Being newer than sequence stratigraphy, the study (Helland-Hansen and Gjelberg, 1994) first outlined the shelf-edge trajectory method in order to provide a more descriptive alternative to notoriously inexplicit sequence stratigraphic interpretations. According to the authors, trajectory analysis views the depositional system in a continuously evolving frame of reference while involving a more objective methodology; requiring less 'a priori' assumptions. In other words: trajectory analysis is a spatially continuous, high resolution, explicit method that complements and extends upon conventional sequence stratigraphy. Clinoform trajectory analysis is now considered to be a significant advancement regarding this topic (Catuneanu et al., 2009).

Burial, differential compaction and isostatic subsidence

Eroded sediments are transported to the basin where they bury older strata and expel pore-fluids, causing compaction. The resulting reduction in the buried rock's porosity coincides with a loss of volume. Elastic and plastic compression of sediment grains and trapped pore fluids account for an additional, small fraction of volume loss in sediments after burial (Hantschel and Kauerauf, 2009). Shaley sediments contain mostly fine-grained, flat clay grains while sandy sediments mostly consist of coarse grained and rounded sand grains. Initially, the porosity of sands and shales is around 50 to 60% with clay-rich sediments being significantly more porous than sand-rich sediments (Sclater and Christie, 1980; Baldwin and Butler, 1985). During compaction however, individual clay plates tend to imbricate, resulting in the sealing of pore throats and a large loss of volume. In contrast, the larger more rounded sand grains hold open pores and lose less volume when compacted. For these reasons, clay-rich shales are compacted more than sandy sediments in case of equal burial (Revil et al., 2002). Thus, strata that have laterally discrepant ratios of sand versus shale are subjected to differential or unequal compaction. Since clinoforms generally have more coarse-grained sandy

material in the landward compartments and more fine-grained, shaley sediments in the basinward compartments, compaction of buried clinoforms is differential and thus distorts primary, syn-depositional clinoform trajectory orientations, thus affecting interpretations.
Another significant effect that occurs parallel to compaction is isostatic subsidence of the crust (Vink et al., 2007; Blum and Roberts, 2009). Given enough mass and time, sediments that weigh down on underlying strata overcome the rigidity of the lithosphere. As a result, strata are depressed with respect to eustatic sea-level (relative to the centre of the Earth). Shelf-edge deltas and clinoforms are large enough to bring about isostatic subsidence (Blum and Roberts, 2009). Therefore, clinoform trajectories are also distorted by isostatic subsidence.

Aim

The aim of this study is to correct shelf-edge trajectories for compaction, differential compaction and isostatic subsidence by accounting explicitly for lithological variations along clinoforms. In doing so, the primary, syn-depositional geometries and trajectories can be reconstructed. This allows to assess the extensiveness of the geometric distortion caused by differential compaction and isostatic subsidence and the impact of these factors on shelf-edge trajectory analyses and the associated observations and interpretations of relative sea level, slope processes, sequence stratigraphy, sediment bypass and the basin fill's response to eustatic signals.

Clinoforms and clinoform successions

Clinoforms are defined as 'ubiquitous, shallow-marine and continental-margin depositional morphologies, occurring through a range of scales' (Patruno et al., 2015a). Originally defined as a 2-dimensional sigmoidal shape in dip-section (Rich, 1951), the term has evolved to refer to: (1) geometrically: a three-dimensional sigmoidally shaped volume. (2) lithologically, prograding basinward fining strata located on the interface between marine and continental lithologies (Patruno et al., 2015b). In all cases, the concept defines a common motif in sedimentary basins that is ubiquitous throughout time-orders (table 1). They are fractally organised in spatial hierarchy (Straub and Pyles, 2012). Meaning; clinoforms exist on different scales and are themselves constructed of smaller clinoforms.
Individual clinoforms are commonly but not exclusively bound by strong reflectors in seismic data or a distinct signature shift in well data. These strong reflectors and signature shifts signify geologically significant demarcations, namely that of a transgressive surface, flooding surface or sequence boundary. These features in turn define clinoforms as individual episodes in the genetic development of the basin fill known as sequences, whereby each sequence represents a distinct episode of basin development namely, one relative sea level rise and subsequent fall (Catuneanu et al., 2009).
Clinoform sequences (often referred to as: clinothems) are deposited consecutively over time as the sediment progrades out into the basin. A completed series of consecutive shelf-edge clinoformal sequences in the basin fill is referred to in this study as a shelf-edge clinoform succession; alternatively it can be called a clinoform set. Shelf-edge clinoform succession are typically tens to hundreds of kilometres long and are deposited over several million years with each sequence representing a unit of time of or fourth order; 100,000s of years (table 1). Shelf-edge clinoform sequences of larger, third order scale may also be called sequences (Vail et. al 1977).
Typically, ancient clinoform successions are imaged on seismic or well log correlation panels. These ancient systems are commonly buried below 1000s of meters of overburden.

Sequence order	Cycle period in Ma	Thickness in m	Stratigraphic name according to this study	Process
First	200-300	10,000+	Megasequence (not considered in this study)	Supercontinent cycle (Wilson cycle)
Second	10-80	1000-10.000	Megasequence (not considered in this study)	Orogenies
Third	1-10	100–1000	Sequence	Orbital eccentricity cycles
Fourth	0.1-1	10–100	Sequence	Orbital eccentricity cycles
Fifth	0.01–0.1	1–10	Parasequence (often called cyclothem)	Orbital precession, obliquity and eccentricity cycles

Table 1. Sequence hierarchy according to (Vail et. al 1977).

Shelf-edge trajectories can be measured sequentially, whereby each individual increment is bounded on either side by a rollover point picked on a strong reflector of lower order. Thus, one sequential increment delimits the trajectory's length within a sequence, signifying a single event of discontinuous sea level rise and subsequent fall within which lower order variations occur (Vail et al., 1977). The reason for this measuring methodology threefold: 1) to maintain accuracy throughout measurements. As mentioned previously, rollover points are most accurately placed on strong reflectors 2) To support consistency, since sequences of a certain time order denote roughly equal time increments (table 1). 3) Record additional insights that are relevant to the process regime surrounding the shelf-edge: Sequential trajectory length provides valuable information because they indicate the total volume of the sedimentary prism infilling the basin (Jones et al., 2015).
4) Each single sequence embodies a motif that signifies part of a cycle in shelf-edge development. Therefore, it serves as a logical and geologically sensible starting point for measurements and observations.

Shelf/slope clinoform rollover points

The clinoform rollover point, sometimes called the clinoform knick-point, refers to a specific point on the surface of a clinoform. Like the term clinoform, there is both a geometric and a lithological definition.

Geometrically, the point is simply defined as the break in slope (Steel and Olsen, 2002). Since consistency in clinoform rollover point determination is important, a more specific definition is considered; mathematically *the rising maximum of the second derivative of the sigmoid that defines the surface of the clinoform* (figure 1). In lieu of a mathematical representation of this surface, a graphical approach is considered: *the rollover point has the shortest (perpendicular) distance from the intersection between extensions of the steepest and the shallowest lines on the slope of the clinoform and the surface of the clinoform* (figure 1). The primary shape of a clinoform is often affected by allogenic processes, most dominantly faulting, tectonic stresses, fluvial incision and other processes of sediment reworking. It is therefore appropriate to consider a restored, simplified version of a clinoform when determining the rollover point by means of its geometry thus disregarding small-scale geometric and post-depositional features.

It should be noted that the term 'inflection point' is often used in reference to the rollover point, yet the inflection point of a sigmoid in fact refers to the steepest point of the curve rather than the break in slope. The inflection point is defined as: *the maximum of the fist derivative of the primary clinoform* (figure 1).

Lithologically, the rollover point refers to a zone (J.Dixon and Steel, 2012). This zone is sometimes referred to as the shelf-break zone, defined as an area that is susceptible to storm wave and tidal reworking and is therefore located in proximity to both the shelf and the sea surface. It is located around the geometric shelf-edge rollover, where there is a marked fining of the sediments and the highest proneness of incision along the shelf (Flint et al., 2011).

On the 5^{th} order scale (table 1), the condensed section that forms at the maximum flooding surface is often the most easily identifiable layer of the clinoform and also signifies a relevant position in a sequence stratigraphic framework (Galloway, 1989). For these reasons, rollover points are commonly positioned on this layer when identifying larger 4^{th} order shelf-edge trajectories. To benefit consistency in measurements, only the geometric definition of the rollover point is considered when determining clinoform trajectories in this study.

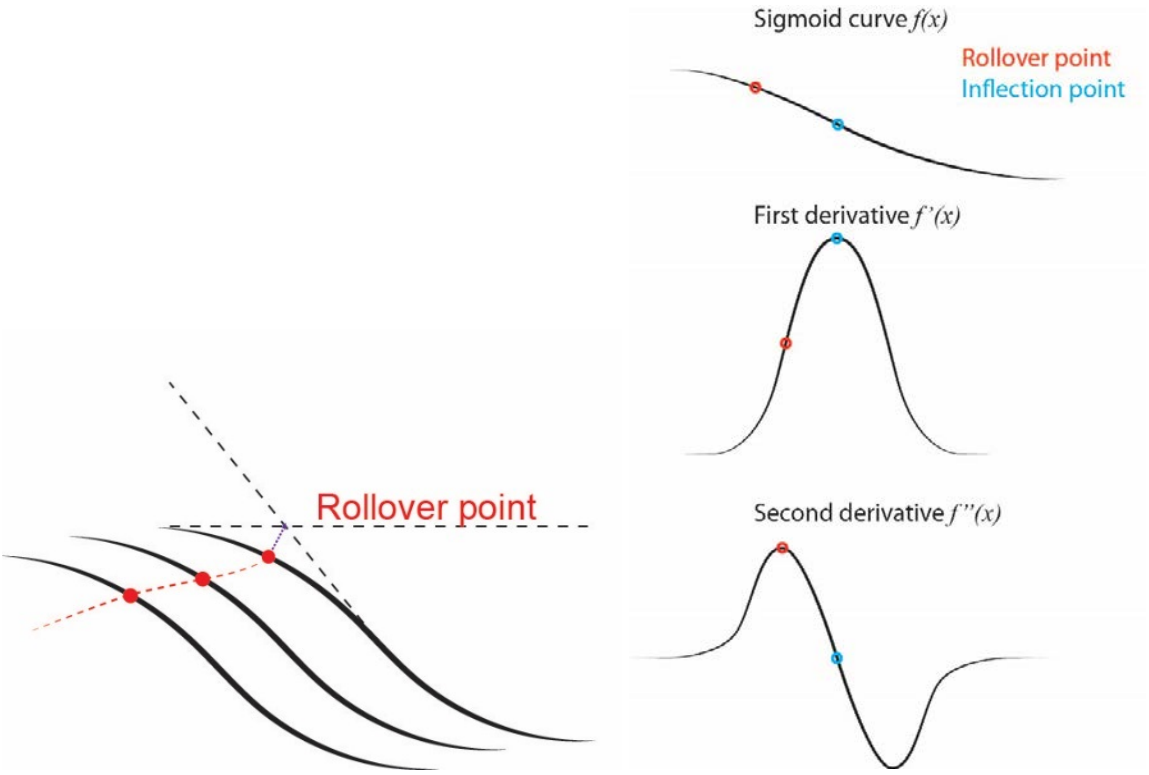

Figure 1. Schematic representation of the clinoform rollover point as it is defined in this study. Geometrically, it is defined as the point that has the shortest (perpendicular) distance from the intersection between imaginary extensions of the steepest and the shallowest lines on the slope and the surface of the clinoform. Mathematically, it is the rising maximum of the second derivative of the sigmoid curve that defines the surface of the clinoform.

Trajectories, stacking patterns and stratigraphy

Since the rollover point of 4th order clinoforms was formed in relative proximity of the sea-surface, along-dip movements of this point are linked to movements in relative sea level. Correspondingly, trajectory orientations and gradients form a record of relative sea-level changes in the stratigraphy (Henriksen et al., 2011). Trajectories track rates of progradation (horizontal/diagonal stacking) and aggradation (vertical stacking) and thereby illustrate stacking patterns. Thus, flat trajectories signify progradation dominated systems while steeply rising trajectories having a larger component of aggradation. In other words; syn-depositional clinoform trajectories are proportionate to ratios of progradation and aggradation (Gong et al., 2015a).

In terms of systems tracts, trajectories are descending in forced regressive strata and flat to rising in normal regressive strata (Burgess and Prince, 2015; figure 2). Similarly, they are landward in transgressive strata and basinward in regressive strata. Trajectories therefore indicate sediment supply and changes in relative sea level. Therefore, they describe a record of the interplay between the two fundamental parameters of sequence stratigraphy; accommodation and sediment supply (Henriksen et al., 2011, Ainsworth et al., 2008, Muto and Steel, 1997). Trajectories can therefore be linked to systems tracts as defined by conventional sequence stratigraphic definitions (Catuneanu, 2006; figure 3; table 2). For example, during deposition of the highstand systems tract (HST), sediment supply exceeds the rate of accommodation. As a result, strata stack in a normal regressive pattern whereby the amount of aggradation is gradually lowered as relative sea level rise is reduced. The corresponding trajectory traces a concave upward path (progradation with a gradually lowering

component of aggradation), (Catuneanu et al., 2009; Figure 3). Similarly, other styles of interplay between accommodation and sediment supply are illustrated by the trajectory's gradient; orientation and trend e.g. concave or convex (figure 3).
The concept of clinoform trajectories can be applied to clinoforms on shoreline/delta scale (5th order), and shelf-edge or shelf-margin (3rd or 4th order) scale. Whereby shoreline clinoforms are usually in the order of 10's of meters in height while shelf-edge clinoforms are in the order of hundreds of meters in height (Johannessen and Steel; 2005; Vail et. al 1977; table 1). This study focusses on clinoform trajectories on the shelf-edge scale, hereafter referred to as: (shelf-edge) trajectories. On both scales however, the technique has similar descriptive, analytic and predictive potential (Helland-Hansen and Martinsen, 1996).

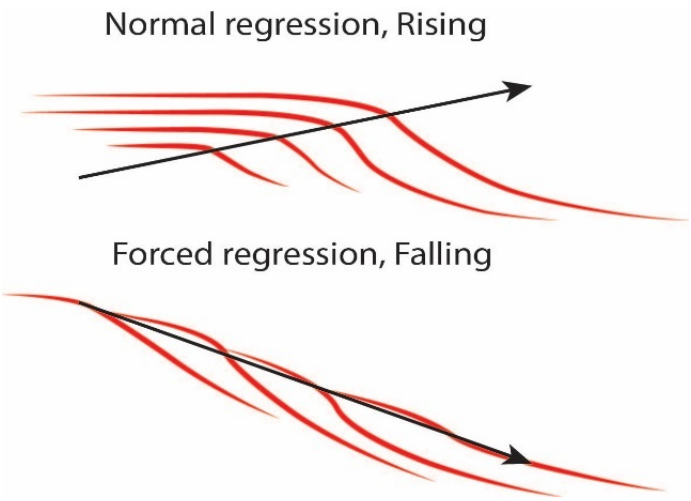

Figure 2. Shelf-edge trajectories are descending in forced regressive strata and flat to rising in normal regressive strata.

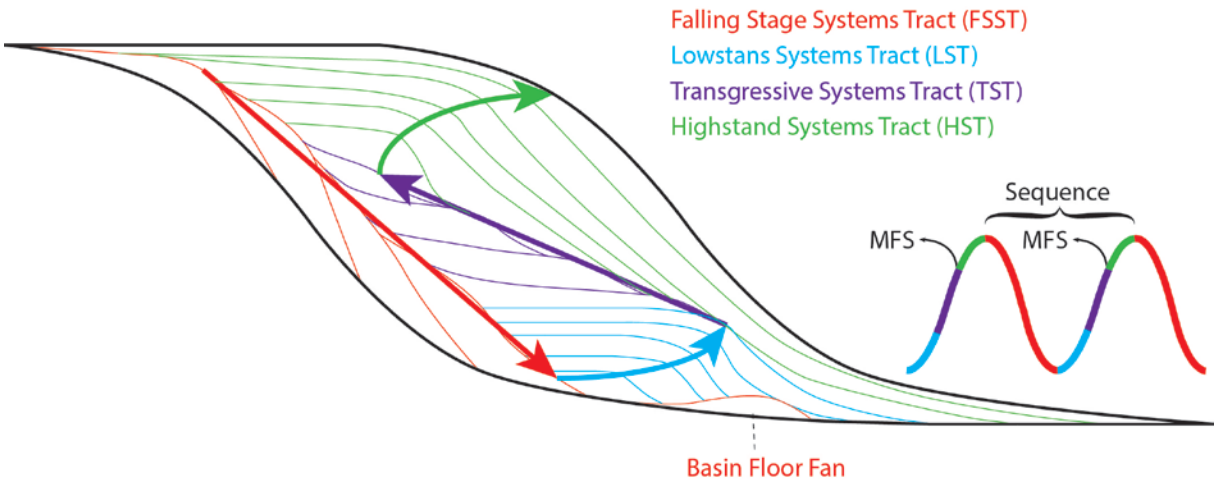

Figure 3. Systems tracts defined by shoreline trajectories. MFS=maximum flooding surface.

Shelf-edge trajectory orientation	Stacking pattern	Genetic type of deposit	Associated systems tract	Note
1. Falling	Progradation	Forced regressive	FSST	Associated with abundant sediment bypass
2. Straight	Progradation	Normal regression	HST+LST	
3. Rising (concave)	Aggradation+Progradation	Highstand normal regression	HST	
4. Rising (convex)	Aggradation+Progradation	Lowstand normal regression	LST	
5. Retrograde	Retrogradation (backstepping)	Transgression	TST	Uncommon on shelf-edge scale

Table 2. Trajectory orientation, pattern stacking and position in a sequence stratigraphic framework in accordance with (Galloway, 1989).

Clinoform geometries

Geometric characteristics of shelf-edge clinoforms are used to infer processes surrounding the shelf and deepwater. Notably, slope gradients are associated with triggering and placement mechanisms of turbidites and mass transport complexes (Hampton et al., 1996). This is because models that link submarine landslides or mass transport complexes include values for shear stress based on these syn-depositional slope gradients (Masson et al., 2006). Also, steeper slopes are associated with different types of mass transport than shallower ones.

Also, clinoform heights or amplitudes reflect basin depth and are used to reconstruct paleobathymetry. The rationale dictates that the vertical distance between the rollover point and the basin floor corresponds to the height of the water column and therefore the depth of the basin (Plint et al., 2009). Thus, by measuring trends in clinoform height along a succession, relative sea-level fluctuations can be inferred.

Topset, foreset and bottomset

Typically, clinoforms are separated into three segments, commonly referred to as; compartments. These are: Topset (shelf), foreset (slope) and bottomset (basin floor). The latter can synonymously be referred to as 'toeset'. Lithologically, topset strata contain most sand while the other two segments are clay-rich (Patruno et al., 2015b).

The shelf-edge trajectory approximately delineates the boundary between the topset and the foreset (Steel and Olsen, 2002); the only difference being that the topset/foreset boundary is marked by the lithological rollover definition, while the shelf-edge trajectory is defined by the geometric definition.

This is because top-fore and bottomsets are lithological features. The boundary between the foreset and the bottomset is located at the lower break in gradient known as the rollunder point (Hodgson, 2017, personal communication). This point is essentially the deeper (distal) equivalent of the rollover point. Often, this rollunder point is hard to pick due to slope disruption, incision and lack of a significant break in the lower slope. For this reason, the boundary can alternatively be defined as; the proximal boundary of the most landward deepwater fan deposits.

Topset/foreset ratios

Another defining parameter for clinoform geometry is the topset/foreset (T/F) ratio. It is defined as the relative volume of sediment in the topset, proportional to the combined volume of the foreset and the bottomset (Prince and Burgess, 2013). Note that there is a disparity between the definition of the term foreset in the context of T/F ratios (where it includes the bottomset) and the conventional definition of the term foreset.

T/F ratios are a measure of relative volume. In dip-section, relative surface measurements are treated as a proxy to volumes. The lateral boundaries of the topset and foreset are resolved to maintain consistency in measurements. These are defined as; vertical boundaries at the points where the thickness of clinoform strata becomes roughly uniform or where the strata reach a pinchout. Morphologically, T/F ratios are a measure indicating the relative volume of sediment that is contained on the shelf with respect to the total sediment budget. The parameter has close morphological and statistical links to the gradient of the corresponding shelf-edge trajectory (Gong et al., 2015b).

Sediment bypass

Clinoform trajectories also bear predictive merit towards deepwater sand extensiveness (Gong et al., 2015a; Helland-Hansen and Martinsen; 1996; Dixon et al., 2012).These deepwater sands are coarse-grained, sand-rich sediment deposits located in deep (abyssal) portions of the basin. Thus, they exempt the general basinward fining lithological trend of clinoforms. They are typically deposited as basin floor fans (Catuneanu, 2002). Basin floor fans are sand-rich, fan shaped, lobate structures deposited in the deep parts of the ocean floor. The formation of these deepwater sands is linked to landward stacking patterns, genetic types of deposits and shelf-edge trajectories. Therefore, trajectories can be used as geometric predictors of deepwater sand extensiveness down the slope. The co-genetic between shelf-edge trajectories orientations and basin floor fans can be explained as follows: Low angle (flat) and falling trajectories are indicative of RSL-fall, which is accompanied with subaerial exposure of the continental shelf. This in term leads to erosion of the lithological shelf-edge rollover zone (Carvajal et al., 2009) and strong development of fluvial conduits that incise and erode the shelf/slope rollover (Stevenson et al., 2015; Dixon et al., 2012). Exposed shelfs supply these fluvial conduits with coarse grained erosion products while they intrude distal areas of the shoreface. This leads to the development of high-density submarine (hyperpycnal) flows that distribute the coarse-grained material to the deeper (abyssal) regions of the basin (Carvajal and Steel, 2009; figure 4). Because of this close co-genetic relation between shelf-edge trajectories and sediment bypass, trajectory gradients are strong, yet understudied predictors of deepwater sedimentation volumes (Gong et al., 2015a). Similarly, T/F ratios bear some degree of predictive merit towards deepwater sand extent (Gong et al., 2015b). Here, the rationale dictates that a large degree of sediment sequestration on the shelf infers underdeveloped hydrological conduits leading to poor sediment bypass and thus, scarce volumes of coarse grained sediments in the deep basin. Hydrological

conduits on the shelf usually come in the shape of fluvial and subaqueous slope channels that are morphologically linked to delta types. Since T/F ratios define delta types, they can be used to predict the system's capacity to bypass sediments to the basin floor (Edmonds et al., 2011).
Part 2 of this study further explores this coupling by establishing statistical links to sequential trajectory gradients, T/F ratios and the extensiveness of deepwater sand deposits.

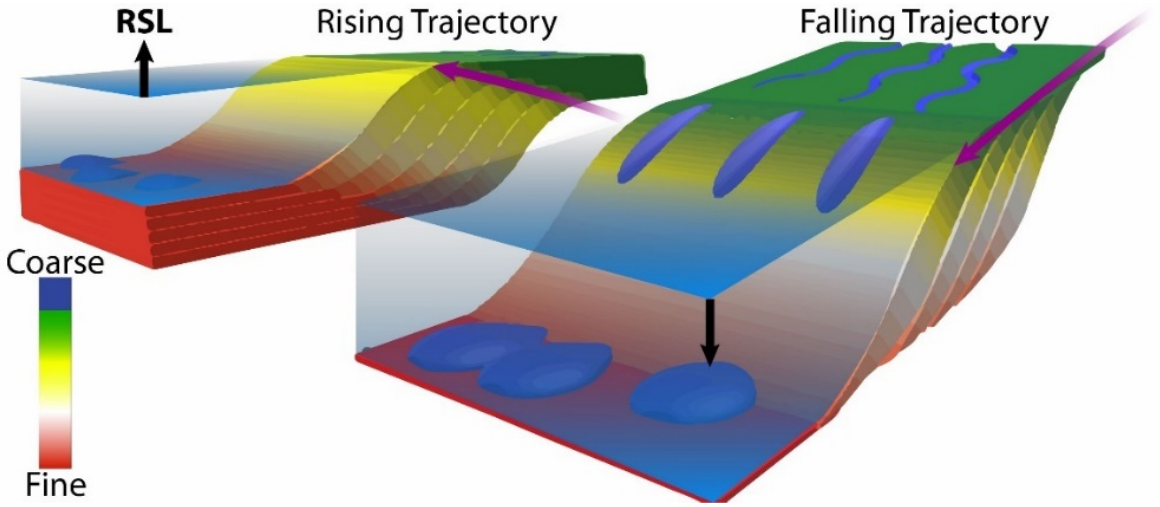

Figure 4. Schematic illustration that shows the differences between high-angle and low-angle (or falling) shelf-edge trajectory systems. The low angle system has better developed fluvial conduits and larger basin floor fans down the slope.

Two phases of decompaction

The decompaction procedure consists of two phases: Phase I): Non-sequential decompaction, followed by phase II): Sequential decompaction. During the first phase, the mass of the overburden that covers the entire succession is backstripped and decompacted. This is a single-step experiment during which the bulk of the overburden that overlies the succession is removed.

Hereafter, phase II): sequential decompaction is applied. During this phase, each clinoform sequence in the succession is backstripped and decompacted successively. Sequential decompaction is thus a multi-step phase. It has to be performed to achieve an accurate reconstruction since individual clinoforms within the succession apply substantial weight on underlying clinoform strata. In other words; each successive sequence buries older sequences, thereby compacting the geometry of the prograding shelf-edge continuously. Thus, to reconstruct the clinoform geometries and trajectories before burial, each individual clinoform sequence needs to be backstripped also.

Sequential decompaction has been applied in previous studies to reconstructed basinal paleobathymetry (Steckler et al., 1999; Deibert et al., 2003). In that study, lithological contrasts for each individual clinoform sequence were not taken into account explicitly, thus differential compaction was not adequately accounted for. Also, sequential decompaction was not used to infer syn-depositional clinoform trajectories. Thus the approach presented in this study is novel and better accounts for differential compaction than previous studies.

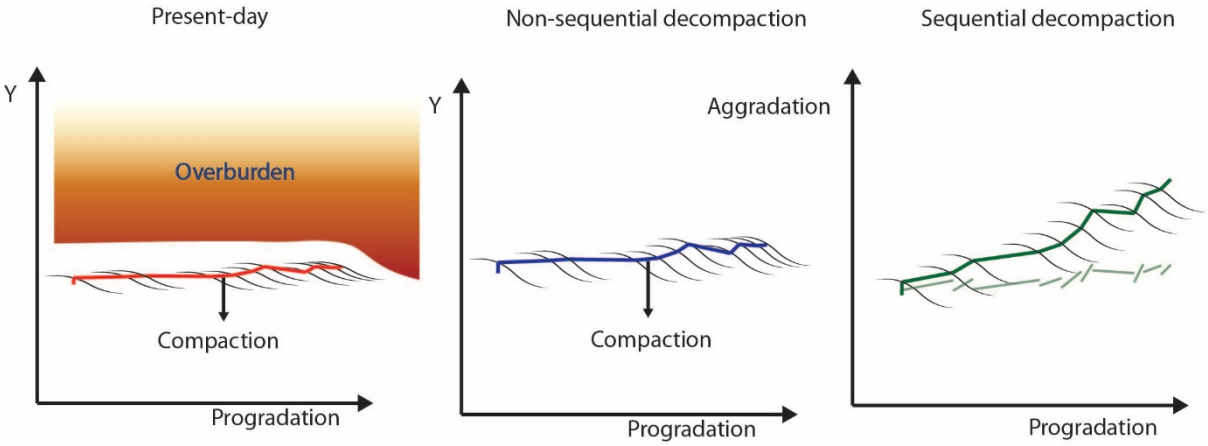

Figure 5. Schematic diagram showing the difference between non-sequential and sequential decompaction. Because the sequentially decompacted system most accurately represents the trajectory angles in their syn-depositional state, the values on the axes are consistent with rates of progradation and aggradation. On the other profile, the trajectory is continuously distorted by (differential) compaction and isostasy. Washakie Basin (Carvajal and Steel, 2012a).

Trajectory incrementation

During sequential decompaction, the trajectory is reconstructed in multiple steps, whereby each step coincides with the reconstruction of a single clinoform sequence. After each step, the trajectory position, gradient and orientation for the reconstructed clinoform sequence is recorded. After each clinoform sequence in the succession has been backstripped, the trajectory forms isolated increments that each represents a single, sequential trajectory increment that has been reconstructed to its primary, syn-depositional orientation. Increments do not match to form a

continuous trajectory because there is continuous compaction and subsidence after the deposition of each consecutive sequence. Therefore, to finalize the reconstruction of the complete trajectory sequential increments are assembled end-to-end (figure 5). Note that the resulting trajectory has never existed in-situ, rather it displays the trend that it would follow if there was no (differential) compaction or isostasy. It is therefore the only objective standard for the proportional measure of progradation versus aggradation and is the most appropriate for interpretation of stacking patterns.

Decompaction models

Images of shelf-edge successions are selected from literature. These form the template for a decompaction model that is input in Midland Valley's Move software. The topset, foreset and bottomset compartments for each sequence are defined. A lithology consisting of two components: sandstone and shale is designated for each compartment. The percentile portion for each of these components is used to calculate the rock density and establish a porosity/depth curve in accordance with (Sclater and Christie, 1980). This relation is: $f = f_0(e^{-cy})$ Where f is present day porosity at depth, f_0 is the porosity at the surface, c is the porosity-depth coefficient (km^{-1}) and y is depth.
100 equally spaced, one-dimensional vertical columns along the succession are constructed. After a selected overburden is backstripped, volume increase is calculated by upscaling the length of the columns based on reducing porosity loss in accordance with the porosity/depth relation. It is assumed that all loss of volume caused by burial is due to porosity loss, elastic properties of the sediment grains and pore fluids are ignored.
The decompacted vertical distance that is indicated by the columns is translated into a surface. This is done by interpolating a polygon between the decompaction columns and several constructed horizons. These horizons represent significant stratigraphic surfaces including flooding surfaces or sequence boundaries. The resulting two-dimensional grid is projected on the dip-section template, modifying it accordingly.
When necessary, the number of columns can be adjusted to overcome inconsistencies such as artefacts and irregularities that are not geologically sensible.
Isostatic adjustment due to unloading is calculated through applying an Airy isostasy (Airy, 1856). Hence, the flexural rigidity of the crust is ignored. The following relation is applied:

$$Z = \frac{S - (H1 - H2)\rho_c - \rho_w}{\rho_m - \rho_w}$$

Where *Z* is the amount of subsidence (relative to a basement datum), *S* is the thickness of the unloaded sediment. *H1* is crustal thickness before sediment load, *H2* crustal thickness after sediment load. ρ_c ρ_m and ρ_w are the densities of crust, mantle and water respectively.

Determination of porosity/depth relations

Sand/shale ratios (V_{shale}) denote the relative contribution of sandstone versus shale, assuming a two-component clastic lithology. Average values for each top, fore and bottomset compartment in the succession are obtained from literature.
Sand/shale (V_{shale}) ratios are derived directly from measurements published in literature, or they can be estimated indirectly from well-log data or outcrop logs. Well logs that show the relative proportion of sand versus shale are obtained from literature (Carvajal and Steel, 2012; Salazar et al., 2016; Johannessen et al., 2011). These values are turn derived from proxies for porosity and minerology like gamma, resistivity, sonic, density and spontaneous potential measurements. An approximation of the V_{shale} ratios can be derived by calculating the ratio between the surfaces on

either side of the measurement curve. This is done by importing the log as a raster image and counting the pixels on either side of the curve. Counting is automated by using the magic wand tool in Adobe Photoshop (Young, 1998) followed by the generation of a histogram that displays the number of selected pixels. Using a similar technique, V_{shale} values can be estimated from published images of outcrop descriptions. In this case, the relative surface area (number of pixels) of sand-rich structures is compared to the surface area of clay-rich structures.
Selected logs transect the full extent of lithological variations in the succession in order accurately determine contrasts in topset, foreset and bottomset lithologies. Data in between log measurements is extrapolated along-dip in the succession. Accurate models have a higher number of log inputs in the dip direction. This is because more logs allow for better normalization for local anomalies and basinward variations in lithology.
It should be noted that different depositional fabrics of clay and silt mineralogies result in a wide spectrum of sorting arrangements and initial water content of the deposits and thus, in different compaction behaviors (Potter et al., 2005). However, the key driver for differential compaction is the basinward lithological fining in natural clinothems. This exists regardless of one chooses to implement simple or more complex lithologies.

Maximum depth of burial

The bulk of compaction is consolidated and is therefore irreversible (Lemée and Guéguen, 1996; Revil et al., 2002). Thus, the maximum extent of the overburden needs to be determined and input into the model. This maximum burial can either be present now (in which case there is no uncertainty) or alternatively, it was present sometime in geological history. In the second case; the maximum burial can be estimated by means of studying the history of the geological setting and identifying episodes of overburden accumulation and episodes of uplift and erosion. In some instances, such as with the Karoo datasets, apatite fission track data was obtained and used to estimate the maximum depth of burial (Linol and de Wit, 2016).
Determining the maximum depth of burial for some datasets presents modest uncertainties. Since there is limited distortion in non-sequential decompaction, these uncertainties do not substantially diminish confidence in the results.

Workflow

A bitmap image template from a selected dataset forms the basis for the decompaction model. They show 2D raster images of dip-oriented prograding shelf-edge clinoform profiles that are constructed from outcrop, seismic or well-log data. In case the templates do not display the full extent of the overburden, additional overburden is added to conform to the basinal setting of the succession. Templates are depth converted if necessary.
Horizons are constructed to demarcate sequence boundaries. Next, two laterally conformable horizons are constructed to divide sequences in a topset, foreset and bottomset compartment. These two horizons are 1) roughly equal to the shelf-edge trajectory, bounding the topset and the foreset region. 2) Roughly equal to the rollunder trajectory, bounding the foreset and the bottomset. In all cases, the interpretation honours that of the published dataset from where the template is obtained. This includes the location of the shelf-edge trajectory which is drawn from rollover to rollover, thereby ignoring trends within sequences. In case the trajectory is not included on the image template, rollover points are picked methodologically, in accordance to the aforementioned geometric definition (figure 1).

A decompaction model is constructed by building a polygon on each individual topset, foreset and bottomset compartment within the succession. Next, V_{shale} values are obtained from literature and specified for each polygon.
After decompaction, present-day, non-sequentially decompacted and non-sequentially + sequentially decompacted trajectories are superimposed in a decompaction overview which allows for the evaluation of the extent of (de)compaction.
Finally, sequential decompaction experiments are compiled in compaction videos that illustrate the development of the clinoformal basin fill trough space and time. These videos therefore show a simulation of the response of clinoforms and their associated trajectories with regards to compaction, differential compaction and isostatic subsidence. Videos (.mp4) are included in the appendix (appendix 4). Additionally, there is an image depiction of the worklow in the appendix (appendix 2).

Datasets

A total of eight outcrop, well log and seismic datasets that illustrate prograding shelf-edge successions are selected to illustrate a wide spectrum of examples (figure 6; table 2). Datasets are from a range of basinal settings and cover a variety of lithological makeups and shelf-edge trajectory styles.

Google Earth (.kmz) files containing the exact location of transects along with a referenced bitmap image of the model template are included in the appendix (appendix 1).

	Data type	Country	Succession age	Notes	Template Reference
1. Washakie basin	Well-log	United States (Wyoming)	Maastrichtian	Best lithological control. Two panels	(Carvajal and Steel, 2009, Carvajal and Steel 2012)
2. van Keulenfjorden	Outcrop	Norway (Svalbard)	Eocene	Imaged on both well log and seismic data. Good lithological control	(Steel and Olsen, 2002)
3. Exmouth Plateau	Seismic	Offshore Australia	Late Jurassic/ Early Cretaceous	Well data down-dip of succession.	(Reeve et al., 2016)
4. Karoo	Outcrop	South Africa	Late Permian	Ancient system, very large overburden.	(Jones et al., 2015)
5. Columbus basin	Seismic	Offshore Trinidad/Venezuela	Miocene-Pliocene	Stepped trajectory, bounded by normal faults.	(Chen et al., 2014)
6. Sarawak basin	Seismic	Offshore Malaysia (Borneo) note: claimed by China (PRC)	Miocene-recent	Contains carbonate platforms. Trajectories not considered in this dataset.	(Koša et al., 2015)
7. Taranaki basin	Seismic	Offshore New Zealand	Pliocene	Overall falling trajectory.	(Anell and Midtkandal, 2015)
8. West-Siberia basin	Well log and seismic	Russia	Early Cretaceous	Largest dataset, 550 km long profile. Sequential decompaction not performed.	(Pinous et al., 2001)

Table 3. Datasets; data-type, location, reference and additional information.

Figure 6. Locations of the basins examined in this study 1. Washakie Basin, 2. Van Keulenfjorden 3. Exmouth Plateau 4. Karoo Basin 5. Columbus Basin 6. Sarawak Basin 7. Taranaki Basin 8. West-Siberia Basin. Note, numerical order is based on the dataset's significance in this study.

1. Washakie Basin

The Maastrichtian Lewis-Fox Hills formation is a clinoformal shelf-edge succession deposited in the Washakie/Great Divide Basin in Wyoming, United States. This basin formed during the Late Cretaceous Laramide orogeny when the uplift of several local mountain ranges coincided with the subsidence of several intermontane structural basins (Olariu et al., 2012; Koo et al., 2016). The 100-kilometre succession consists of 16, 4th order sequence-scale clinoforms that were deposited over roughly 1.5 Ma in the Maastrichtian. Subsequently, the Lewis-Fox Hills succession was buried below approximately 3300 m of sediments (Finn and Johnson, 2005). The basin fill concurred with effective coarse grained sediment bypass, leading to the deposition of extensive basin floor fans.
(Carvajal and Steel, 2012) presented a quantitative analysis on the source to sink system in the Lewis-Fox Hills formation in the Washakie Basin. The study details sand/shale ratios deduced using gamma-ray, conductivity and spontaneous potential logs from about 620 wells across the basin. Thus, unprecedented lithological control in the area allows for a very high confidence decompaction model. Since the succession was constricted from well data, there is also an accurate measure for the extent of the overburden.

2. Van Keulenfjorden

The van Keulenfjorden is a bay located on the southern part of the Spitsbergen Island in the Norwegian Svalbard archipelago. The bay's southern facing mountainside contains an approximately 25-kilometer-long 3rd order shelf-edge clinoform succession in outcrop. Eocene sediments were deposited over approximately 6 Ma on a passive margin in Svalbard's Central Tertiary Basin (Johansen et al., 2007). They display 20, 4th order sequence-scale clinoforms which recorded the basinward accretion of coeval, coastal-plain, marine shelf, slope and basin floor lithologies (Johannessen et al., 2011). These uniquely exposed seismic-scale sediments have been researched

extensively for their significance as an outcrop analogue for shelf-edge systems, relevant for studies involving deepwater sedimentation and hydrocarbon exploration (Steel and Olsen, 2002; Plink-Björklund and Steel, 2004). A study involving an integrated ground penetrating radar, outcrop, seismic, well-logging and core data approach has been performed by (Johannessen et al., 2011). It presents an extensive outline of the outcrop's lithological make-up, allowing for high-confidence decompaction.
The succession has been substantially eroded and has lost a portion of its original overburden. Studies on the basinal setting conclude that the extent of this overburden was around 2000 m at its maximum (Nøttvedt et al., 1992).
In addition to the sediment overburden, a substantial glacial overburden was present during the last glacial maximum. Studies have concluded that the ice cap had a thickness of around 1000 meters in this area (Landvik et al., 1998). This additional overburden has been included in the decompaction model.
Sand/shale ratios are determined from a lithological log published in (Johannessen et al., 2008). The log penetrates coastal plain, delta plain, shelf-edge delta, slope, shallow marine, basin floor and distal basin floor fan facies, thus intersecting a complete transit of the succession that includes the full suite of lithologies present in the succession. Additional lithological data from (Grundvåg et al., 2014) further increased confidence in model inputs.

3. Exmouth plateau

The North-western section of the Australian passive margin contains the Exmouth Plateau: A deep-marine platform extending 350 kilometres out into the Indian Ocean. It is bounded by transform faults that delimit two adjoining abyssal plains. Multiple sub-basins on the plateau were created due to crustal thinning associated with depth-dependant extension (Reeve et al., 2016). The Upper Jurassic to Lower Cretaceous Barrow Group is deposited in one such sub-basin. It consists of 65 kilometres of prograding shelf-edge scale delta clinoforms, deposited over 8.5 Ma.

4. Karoo

Outcrops in the Laingsburg depocenter of the Karoo Basin expose a Late Permian prograding shelf-edge succession (Flint et al., 2011). The stratigraphy of this depocenter contains the full range of lithological facies associated with a prograding shelf-edge, from shelf-edge delta to basin floor. This stratigraphy is known as the Ecca Group. Like van Keulenfjorden, the Ecca-group outcrops have been subject of extensive research partly due to their value in hydrocarbon exploration by presenting a surface analogue of a seismic-scale shelf-edge clinoform succession.
A series of East-West trending, gently eastwards plunging folds contain three roughly parallel dip-oriented outcrops termed: Zoutkloof, Baviaans-Noord and Baviaans-South. The following study: (Jones et al., 2015) presents a correlation panel for each of these three outcrops, detailing the lithological makeup of the succession, including position of the shelf-edge trajectory. Decompaction was performed on the Baviaans-North section.
The sediments are now exposed on the surface but were at some point in the geological past buried below kilometres of sediments. Apatite fission track data is combined with geothermal gradient measurements to calculate the maximum extent of the overburden in the past. This was determined to have been around 6300 meters (Hodgson, 2017 personal communication; Linol and de Wit, 2016).

5. Columbus Basin

The Columbus Basin is located within the Eastern part of the larger Venezuela Basin. It is defined by North-West to South-East oriented extensional normal faults. The Paleo-Orinoco shelf-edge succession in the Columbus Basin (offshore Venezuela and Trinidad) consists of clastic sediments supplied by the extinct Paleo-Orinoco river delta system from the late Miocene throughout the Pliocene (Chen et al., 2014).
A dip-oriented seismic profile of the succession shows an unusual stepwise aggradation dominated/progradation dominated shelf-edge trajectory. This pattern is the result of alternating phases of margin accretion and subsidence (Chen et al., 2014). Sand/shale ratios are derived from well logs and outcrop analogue studies.
The following study: (Wood, 2000) integrates seismic and well-log data from the area and outlines general trends in sand/shale distribution. Additional research was performed on a laterally equivalent lithological member of the Paleo-Orinoco shelf known as the Morne l'Enfer member (Peng et al. 2017). This lithological member outcrops on the Southwestern tip of the Island of Trinidad where it comprises of delta-front, shoreface, offshore, and transgressive deposits believed to be analogous to the sediments that make up the Paleo-Orinoco shelf-edge (Chen et al., 2014; Peng et al. 2017). Accurate lithological descriptions of the Morne l'Enfer member including values of sand/shale ratio are outlined in (Bowman and Johnson, 2014).

6. Sarawak Basin

The Central Luconia region of the Sarawak Basin, North of Borneo is an area in the Southern region of the South China Sea marginal basin. It contains extensive Miocene to Holocene carbonate build-ups (Collins 2016, personal communication; Koša et al., 2015). Two deltas coming from the Southwest and the Southeast built out siliciclastic erosion products from the uplifted hinterland (Cullen, 2010). The sediments form a clinoformal shelf-edge succession in which eight regressive cycles can be identified. Hydrocarbon exploration in the area has attracted considerable scientific interest, resulting in extensive literature based on the area's plentiful collection of well-log and 2D seismic data. This material has allowed for an accurate the determination of the sediments' lithological makeup.

7. Taranaki Basin

The Taranaki Basin located onshore and offshore New Zealand is a Cretaceous to Recent multi-phase rift bounded by the reverse Taranaki fault to the East and a complex half graben system to the West (Holt and Stern, 1994). The Giant Foresets formation is a clinoformal succession of shelf-edge scale, deposited over 4 Ma during the back-arc phase of rifting in the Pliocene and Pleistocene (Hansen and Kamp, 2002). Abundant quantities of published data allows for strong control on lithologies (Anell and Midtkandal, 2015). Around 13 sequence-scale clinoforms totalling around 100 kilometres in length are discerned.
Lithological data is derived from (Holt and Stern, 1994) which describes the lithological makeup of the Giant Foresets formation in detail by integrating gamma ray, sonic, density logs, a 1700 km^2 3D and a 4000 kilometre 2D suite of seismic data.

8. West-Siberia Basin

The Lower Cretaceous (Neocomian) complex of central West Siberia consists of a 640-kilometre-long, westerly prograding shelf-edge clinoform succession of Early Cretaceous age (Pinous et al., 2001). It covers 16 giant 4^{th} / 3^{rd} order depositional sequences deposited over 9 Myr in a North-South oriented Triassic rift system. The Basin floor fan system, known as the Achimov formation forms a major hydrocarbon reservoir in the west-Siberia petroleum province; the largest petroleum system in the world, hosting an estimated 144 billion barrels of discovered reserves (Ulmishek, 2003). The thickness of the sediment overburden that covers the succession reached its maximum extent of 2800 meters in the Quaternary (Pinous et al., 2001). The dataset is constructed from 2D seismic and well-log data presented in the study: (Pinous et al., 2001).

RESULTS

Table 3 shows the average gradient of the trajectory for each dataset in addition to the change following decompaction.

	Overburden (from youngest rollover)	Average gradient (°)	Average gradient (°) (non-sequential)	Change (°)	Average gradient (°) (sequential)	Change (°)	Isostatic readjusment (m)
1a. Washakie East	3393	0.27	0.43	0.16	0.69	0.43	1501
1b. Washakie West	3199	0.23	0.42	0.18	0.73	0.50	1592
2. van Keulenfjorden	1527	1.08	1.75	0.67	2.39	1.31	510
3. Exmouth Plateau	1140	1.49	1.77	0.272	2.73	1.237	1085
4. Karoo, Ecca, Baviaans North	6338	0.05	0.29	0.24	0.27	0.21	3341
5. Columbus basin	1644	N/A	N/A	N/A	N/A	N/A	432
6. Sarawak basin	N/A	N/A	N/A	N/A	N/A	N/A	N/A
7. Taranaki basin	742	-0.66	-0.57	0.09	-0.14	0.53	468
8. West-Siberia Basin	3028	0.06	0.08	0.02	N/A	N/A	1506

Table 4. Quantitative decompaction results.

An image overlaying the present-day (red), non-sequentially (blue) non-sequentially + sequentially (green) decompacted trajectories in addition to the image templates used for the decompaction model illustrate the outcomes of the decompaction experiments.
Results from the experiments include a full quantitative account for each dataset in the appendix (appendix 3).

Washakie Basin

There are two roughly North-South trending dip-oriented correlation panels, laterally separated by approximately 15 kilometres (Figure 7, 8). The Western profile runs from sequence 3 to 13 while the Eastern profile is slightly shorter, running form sequence 6 to 13. There is an extremely steep 43° aggradation dominated sequence in the oldest portion of the trajectory. Afterwards, both profiles show a crudely similar, gradually rising shelf-edge trajectory with a flat, progradation dominated increment in the centre.
Because there is substantial overburden in the area, isostatic readjustment exceeds 1500 meters and median gradient exaggeration is 51%. Following sequential decompaction, rotation of the trajectory

substantially exaggerates the rising orientation transforms the flat increment to a rising. The falling increment in sequence C10 rotates from falling to flat.

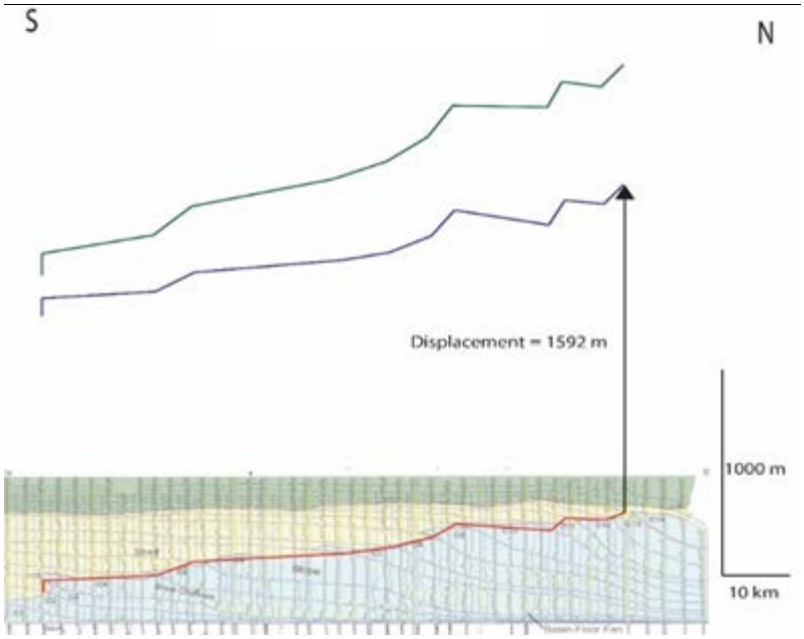

Figure 7. Washakie Basin Eastern Profile.

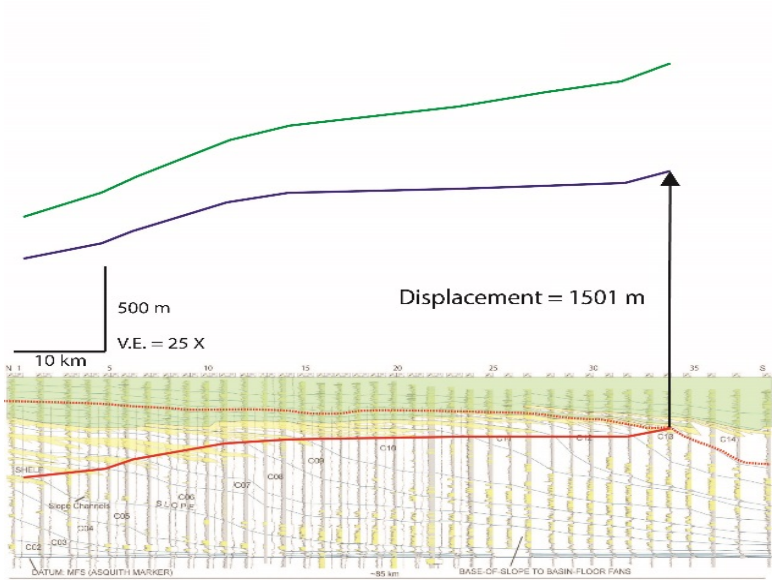

Figure 8. Washakie Basin profiles. Note that the Western trajectory runs from sequence 6 to 13 while the Eastern profile is from 3 to 13 (Carvajal and Steel, 2012a; Carvajal and Steel, 2009).

Washakie Basin: Sensitivity to lithological contrasts

The high-resolution lithological data from the Washakie Basin dataset is obtained from (Carvajal and Steel, 2012). A porosity/depth relation for each top-fore and bottomset compartment in the succession is calculated from these lithological inputs (figure 9). Though there is substantial divergence in the results, sets are consistently grouped together. The topset group has substantially shallower curves than the fore and bottomsets curves, with the forests having the steepest porosity/depth relations. This indicates that with even depth increase (burial), fore and bottomsets lose more porosity than topsets.

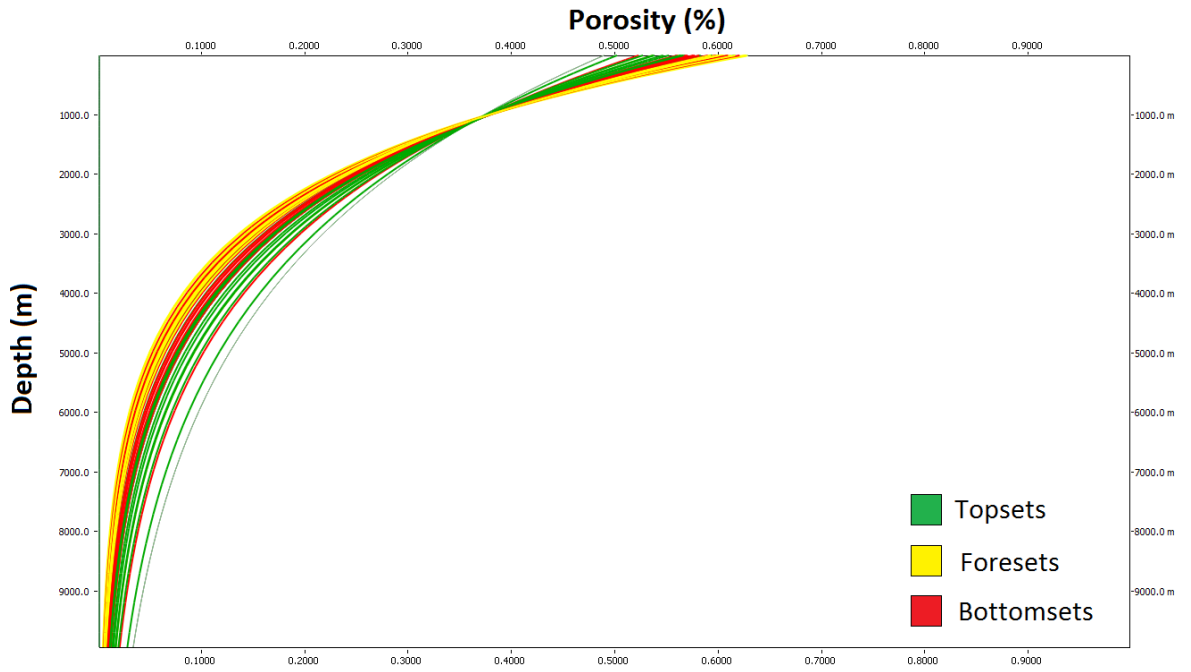

Figure 9. Compartmental porosity/depth curves calculated from V_{shale} ratios, in accordance with (Sclater and Christie, 1980). Example from Washakie Basin decompaction model. Note grouping of top, fore and bottomset compartments. Steeper curves (fore and bottomsets) contain more shale and compact more than sandier topsets in case of equal burial.

This high-resolution data was used to establish the model's sensitivity to lithological contrasts. This is done by negatively and positively slanting the percentage of sand in the Washakie Basin sediments by 10, 50 and 100 percent, totalling 7 separate decompaction experiments. Thereafter, the results of these experiments are superimposed with the unaltered lithological data to identify the differences in results caused by alternative lithologies (figure 10).
There is clear distinction between the results of non-sequential and sequential decompaction experiments. While non-sequential decompaction indicates a very modest difference the results of the experiments. Sequential decompaction illustrates a substantial and moderately consistent variation.

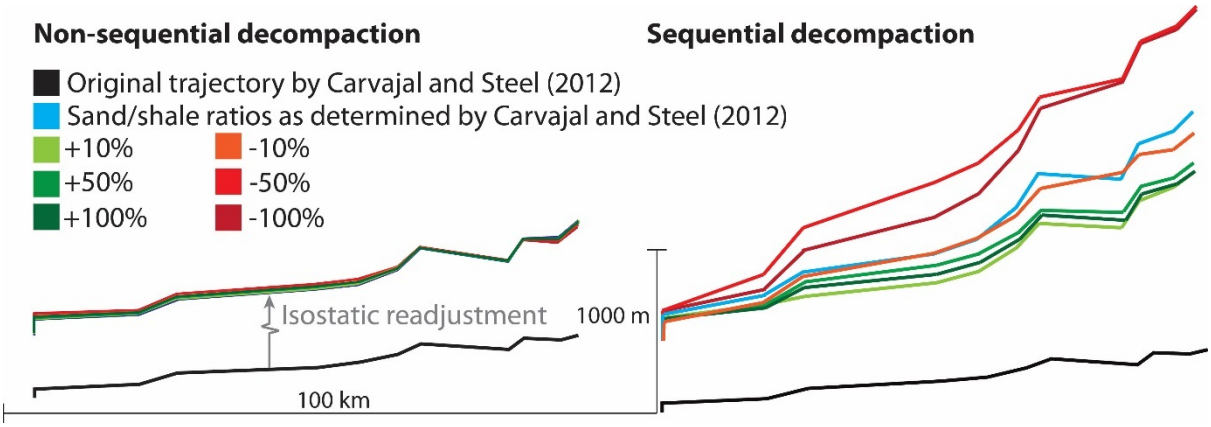

Figure 10. Sensitivity analyses of the decompaction model. High-resolution V_{shale} values where increased and decreased by 10, 50 and 100 percent sand. Thereafter, results are superimposed with the unaltered lithological data to identify the extent of alterations due to diverging lithologies. Note that the non-sequential decompaction has low sensitivity while the sequential decompaction has high sensitivity. Isostatic readjustment not to scale.

van Keulenfjorden

The succession describes an irregular but overall rising trajectory (figure 11). Results of the decompaction indicate; exaggeration of trajectory gradients by an average 38% following the non-sequential decompaction. Sequential decompaction slightly modifies the trajectory, rotating the flat increment in sequence 15 to rising and increasing the overall gradients by an additional 37% with respect to non-sequential decompaction.

The most profound changes however, occur in terms of clinoform morphology. The apparently sigmoidal sequence 8 clinoform is revealed to have an extremely bottom-heavy primary geometry that protrudes downward in a bulge-like morphology, substantially deforming underlying strata. Clinoform deformations are shown in the decompaction video (appendix 4).

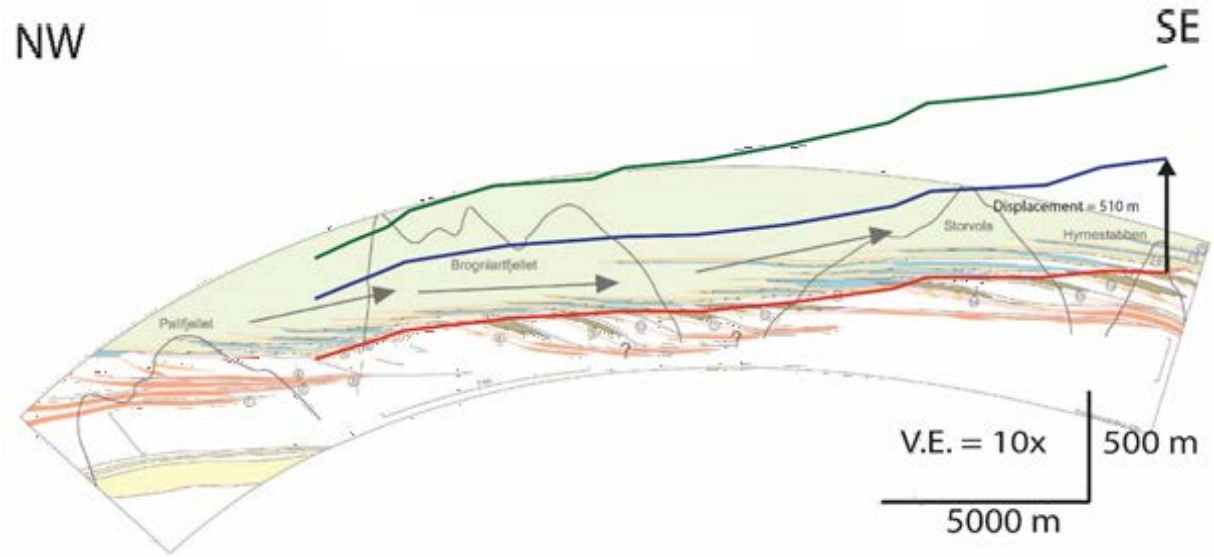

Figure 11. van Keulenfjorden profile (Steel and Olsen, 2002).

Exmouth Plateau

The trajectory describes an overall rising path with a steep section in the middle, ending in a horizontal straight segment in the proximal direction (figure 12). Non-sequential decompaction results in an 850-meter isostatic readjustment and a minor (20%) exaggeration of gradients. Sequential decompaction brings about substantial upward rotation while the proximal straight increment remains intact. Reconstructed clinoform geometries exhibit downward protruding bulges, deformation of underlying strata and reveal several divergent geometries with lowered slope-angles. Removal of the parasitic delta that caps of the succession relieves the distal end of the trajectory, adjusting it from a present day straight orientation to a straight (flat) orientation.

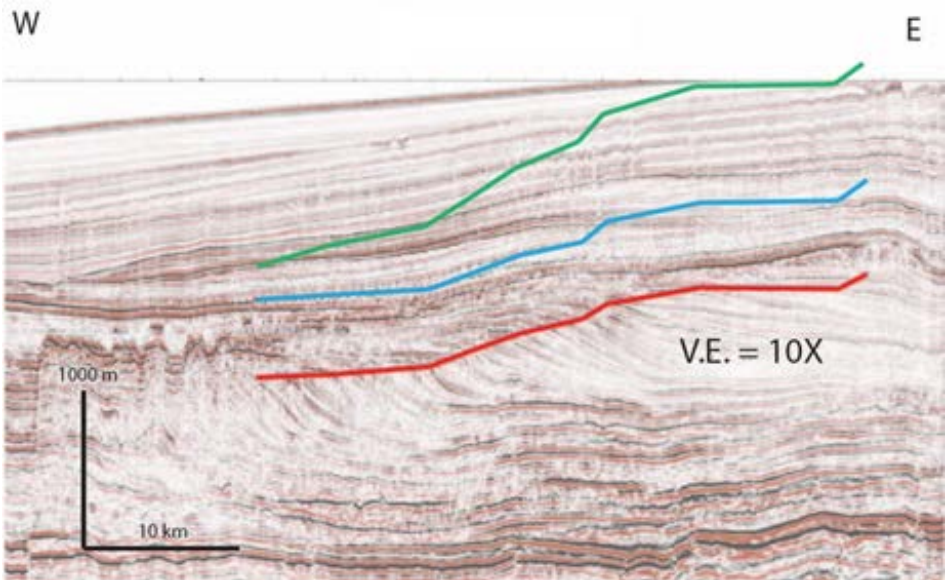

Figure 12. Exmouth Plateau profile.

Karoo, Ecca Group

Removal of the 6300-meter overburden displaces the trajectory significantly. Moreover, trajectory gradients are increased by decompaction. The main observation is that the slightly falling -0.30° distal end of the Baviaans-North profile (wfC 5,6,7,8) is adjusted to a 0.05° flat trajectory (figure 13). Sequential decompaction indicates no significant alteration of syn-depositional clinoform geometries. A third observation is a loss of curvature and general flattening in the geometry of the unit F formation; the oldest formation in the Ecca-group clinoformal succession (Jones et al., 2015).

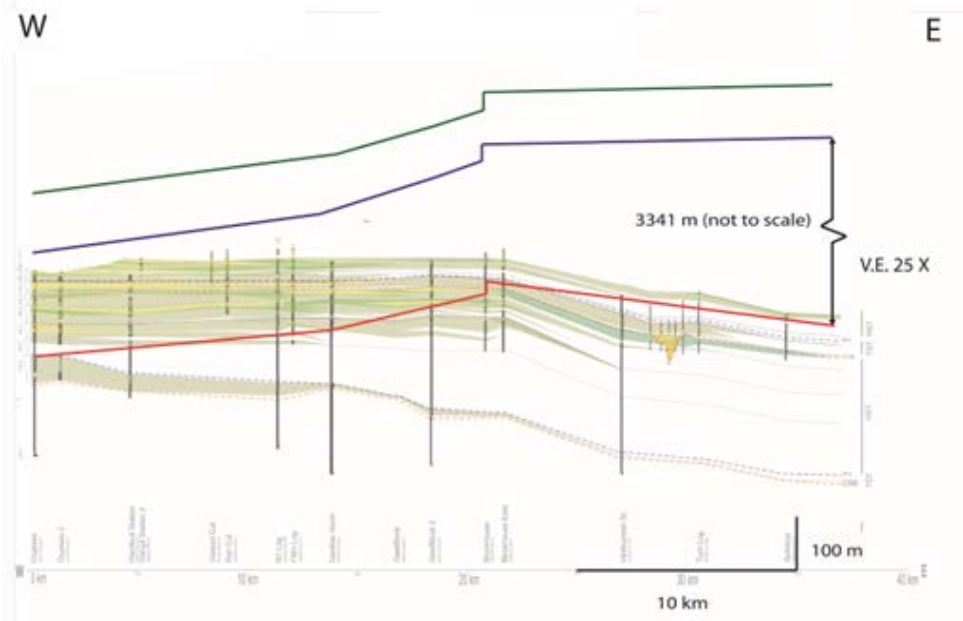

Figure 13. Baviaans North profile (Jones et al., 2015). Note large isostatic readjustment and orientation adjustment of trajectory.

Columbus Basin

The Columbus Basin profile illustrates a stepwise aggradation dominated/progradation dominated shelf-edge trajectory (figure 14). Because there is a limited overburden, there is only a small change in the trajectory following non-sequential decompaction. Sequential decompaction causes an overall

increase in gradient with a downward to upward trajectory adjustment in the fourth sequence of the succession (TP44). Extremely steep sequentially decompacted trajectory intervals indicate extensive aggradation, this is further exaggerated following decompaction. Note that the profile is not depth-converted, this means that the absolute values for trajectory angles cannot he be determined, relative alterations in gradient and orientation after decompaction can however be recognised.

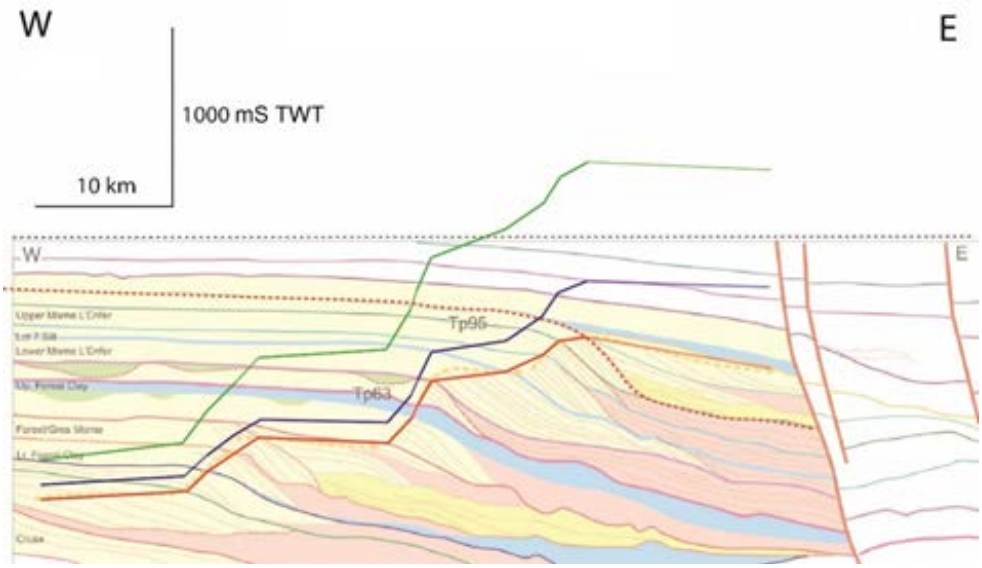

Figure 14. Columbus Basin profile (Chen et al., 2014).

Sarawak Basin

The Sarawak Basin clinoform succession contains several reef platforms that appear to slope downward towards the sea (figure 15). Following sequential decompaction this sea-facing tilt is reduced substantially. Shelf-edge trajectories were not considered in this dataset.

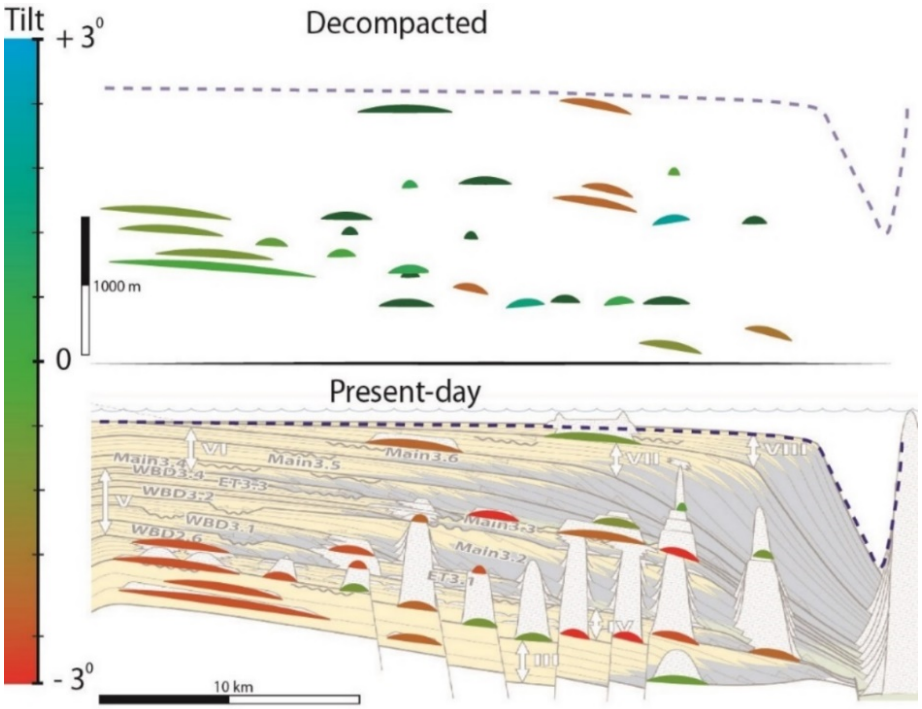

Figure 15. Sarawak Basin profile, note there is substantially less tilting in the carbonate platforms after decompaction (Koša et al., 2015).

Taranaki Basin

The shelf-edge trajectory profile in Taranaki basin has a generally falling trend. A very limited overburden results in modest trajectory readjustment following non-sequential decompaction (figure 16). Despite preservation of the trajectory orientation at the proximal and the distal end, the central part of the trajectory rotates form a seemingly falling trajectory towards an erratically rising trajectory. Though there is no extensive alteration of clinoform geometry, sequential decompaction does indicate extensive deformation of underlying strata and shallower clinoform slopes.

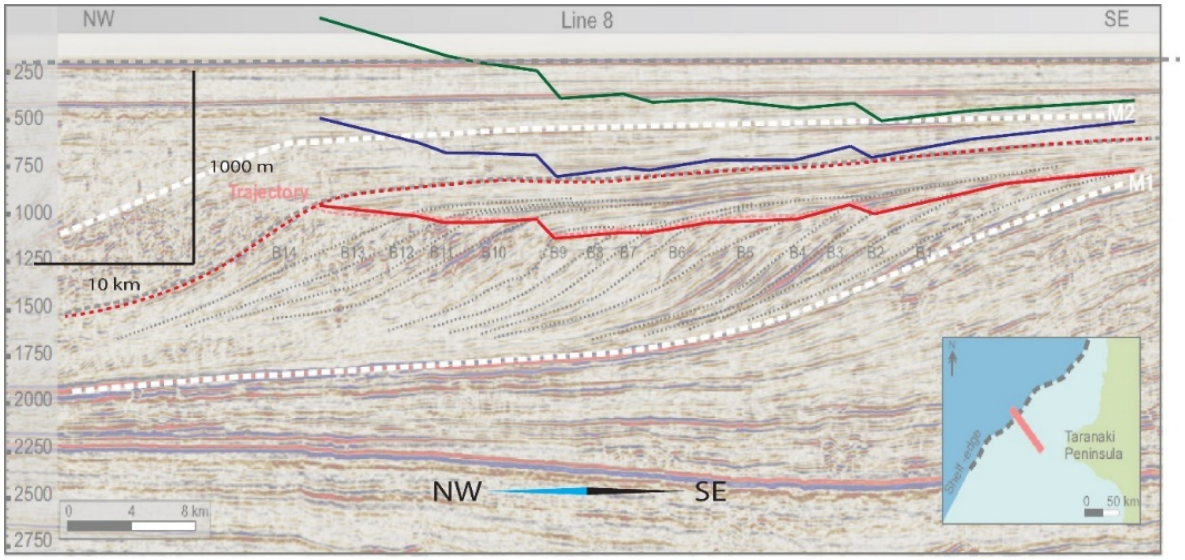

Figure 16. Taranaki Basin profile (Anell and Midtkandal, 2015).

West-Siberia Basin

The succession displays an extremely low-angle rising overall gradient with several falling increments (figure 17). Despite the unusually shallow orientation, gradient exaggeration following sequential decompaction is substantial.

In addition to substantial trajectory readjustment, non-sequential decompaction brings about a gradient exaggeration of approximately 35%. Because the overall gradient is so low, this accounts to a mere 0.02° degree increase in gradient.

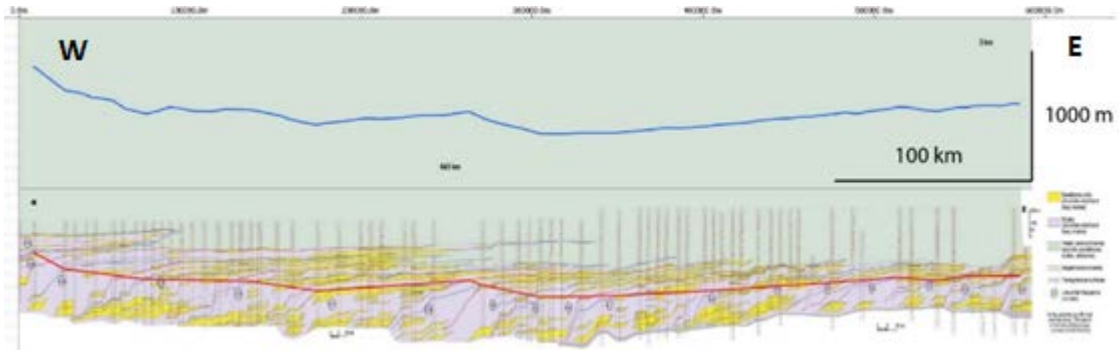

Figure 17. West-Siberia Basin profile. (Pinous et al., 2001). Note the exaggeration of trajectory gradients.

Sea-level reconstruction

Sequential decompaction was applied on the van Keulenfjorden, Washakie Basin and Taranaki Basin datasets. Reconstructed clinoform height and slope gradients were inferred (figure 18). Each data point represents one sequence in the succession. Slope gradients are measured as the average gradient of the foreset surface. Clinoform height is the vertical distance between the rollover point and the basin floor. Note that non-sequential decompaction results in a uniform upwards translation in along-dip trend while sequential decompaction can erratically alters these trends in the Washakie Basin data, often lowering values to below present-day. In the van Keulenfjorden and Taranaki Basin datasets, sequential decompaction results in a uniform downward translation of along-dip trends. Since the most distal rollover point represents the lower boundary of the succession overburden, the results of the most distal sequential decompaction sequence matches with the results of the non-sequential decompaction.

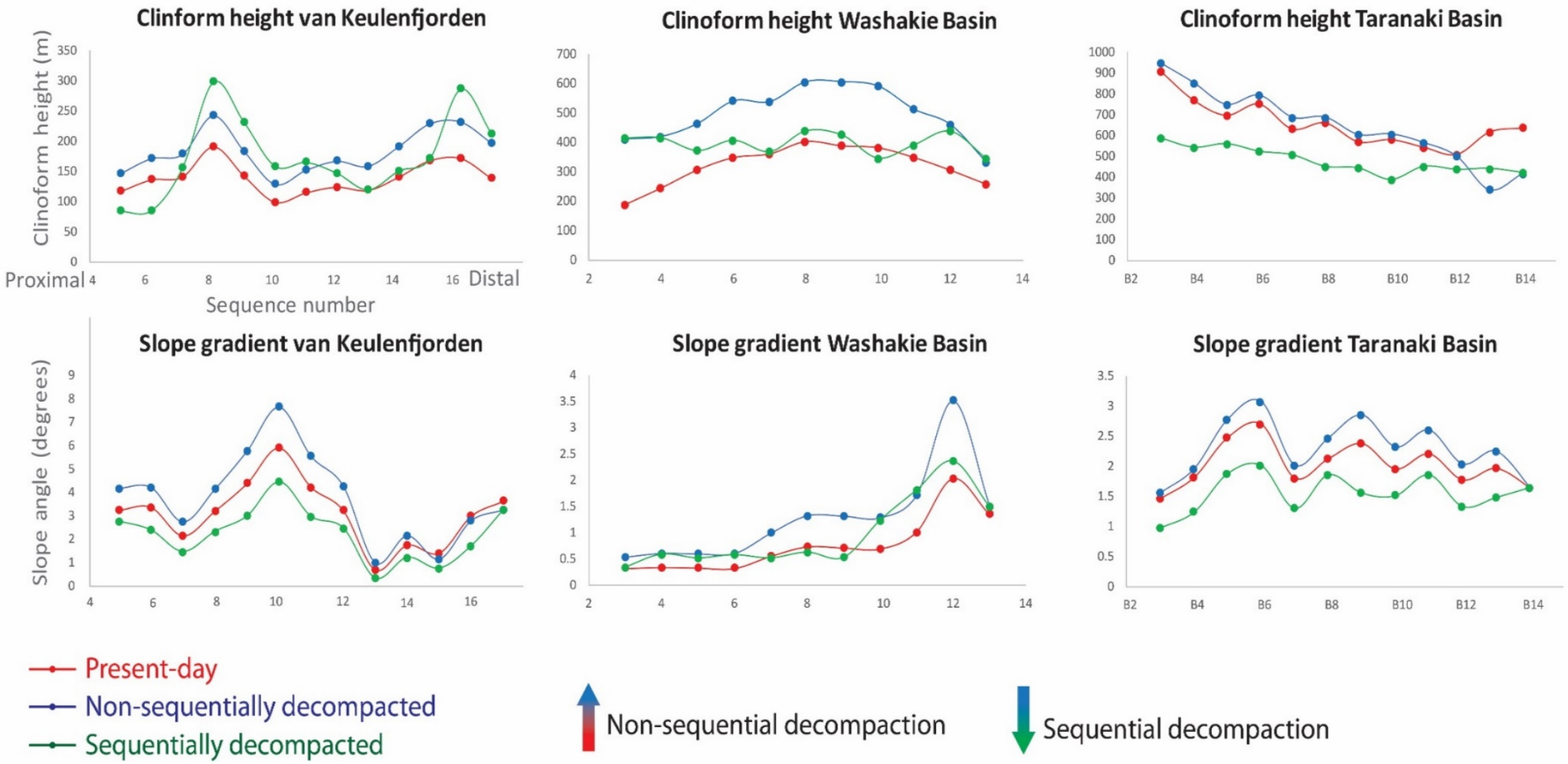

Figure 18. Basinward variations of slope gradients and clinoform heights for outcrop (van Keulenfjorden), well log correlation (Washakie) and seismic (Taranaki) data. Slope gradient is the average gradient surface of the foreset. Clinoform height is the vertical distance between the rollover point and the basin floor. Note that non-sequential decompaction results in a uniform upwards translation in along-dip trends while sequential decompaction erratically alters values (Washakie Basin) sometimes lowering them to below present-day. Basinward extrapolation of lithologies (van Keulenfjorden and Taranaki) results in uniform downwards translation of values.

Two stages of compaction

We recognise two distinct stages in clinothem burial, whereby either stage has a roughly opposite net effect with regards to the geometry of the buried clinothem. These stages correspond to the two phases that are applied in the decompaction procedure. Stage I) sequential compaction, wherein there is major differential compaction; and stage II) non-sequential compaction, wherein there is minor differential compaction. During the first stage, a basinward fining clinothem is buried by a younger clinothem. During this stage, the clay-rich foresets and bottomsets of the buried clinothem compact more than the sandy topsets, thereby causing a basinward rotation of the trajectory and a steepening of the foreset strata, which is accompanied by a vertical extension of the clinothem (figure 4). This vertical extension, in most cases, is greater than the overall compaction, thereby causing a net increase in clinoform height and slope gradient (Green lines in figure 18, figure 19). As the succession progrades further into the basin, older, buried clinothems form sub-parallel belts of similar lithology due to the roughly horizontal alignment of topset, foreset and bottomset compartments (figure 19). The second stage (non-sequential compaction) starts when older, buried clinoform sets in the succession are buried by a simple overburden consisting of horizontally uniform shelf-platform and coastal plain deposits. This causes a largely non-differential compaction that uniformly reduces trajectory gradients and decreases clinoform heights and slope gradients by evenly compressing the buried succession. There is thus an opposition in the net effects of each burial stage with regards to clinothem heights and slope gradients. The reduction of differential compaction after the initial, sequential compaction stage can be seen in our sensitivity analyses, which indicates that while sequential decompaction has a significant sensitivity (figure 10), non-sequential compaction proceeds virtually irrespective of Vshale inputs (figure 10).

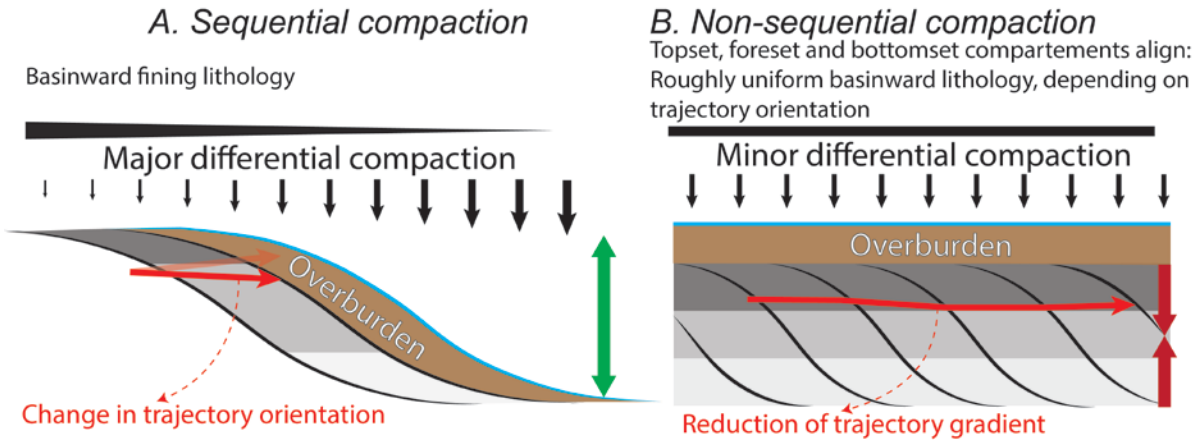

Figure 19. Opposing stages of compaction. Topset, foreset and bottomset compartments are in various shades of grey.

Differential compaction during non-sequential compaction

It should be noted that the reduction in differential compaction due to compartmental alignment is clinoform-trajectory dependent: in the case of perfectly flat shelf-edge trajectories, non-sequential compaction will be completely non-differential. In cases of steeply rising clinoform trajectories, topset, foreset, and bottomset deposits will not be aligned perfectly within the clinothem

successions and therefore lithological heterogeneities will persist down-dip of the succession (Patruno 2017, personal communication). When this is the case, differential compaction continues during non-sequential compaction, but will be much less prominent, as indicated by the results of our sensitivity analyses which were performed on a rising trajectory succession (figure 10). Also, as indicated by the compaction curves most porosity loss and thus, differential compaction occurs in the early, sequential stage of compaction (Fig. 1B). As compaction reduces pore space, the compaction curves converge and differential compaction is reduced accordingly (Fig. 1B).
As more overburden accumulates, porosity is gradualy depleted. Therefore, proportionally less compaction of the succession occurs with further burial. This proportionaly is similar to the porosity /depth relations that were used in the decompaction model (Graph 2). Additionally, there is an isostatic readjustment of the succession that is roughly linearly proprtional to the height of the overburden (Graph 1).

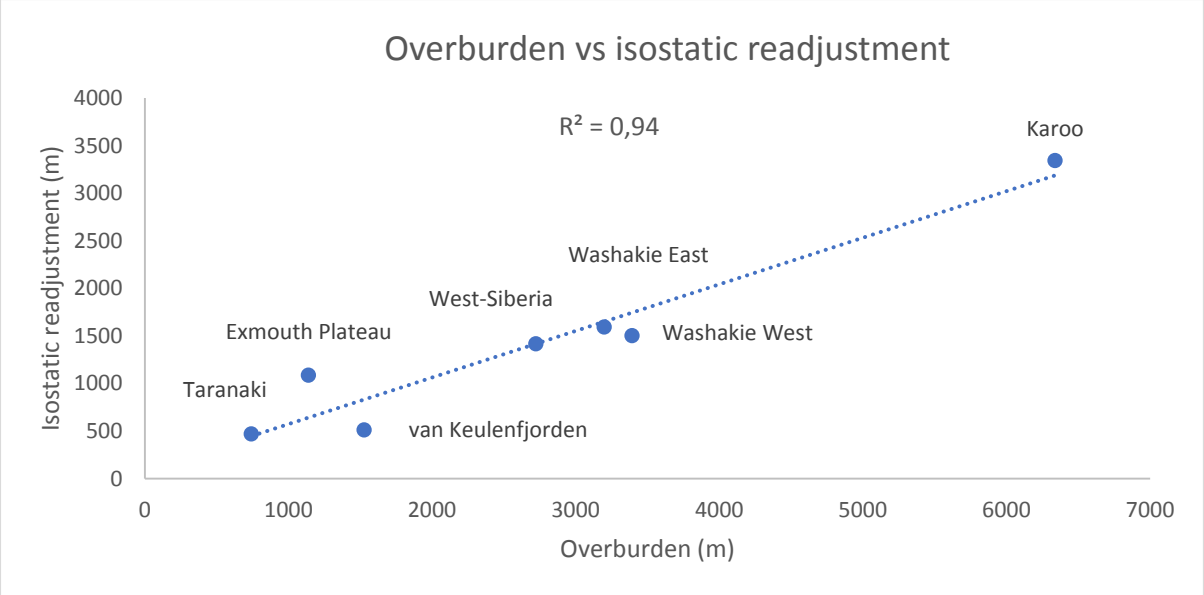

Graph 1. Linear fit between the extent of overburden and isostatic readjustment of the trajectory.

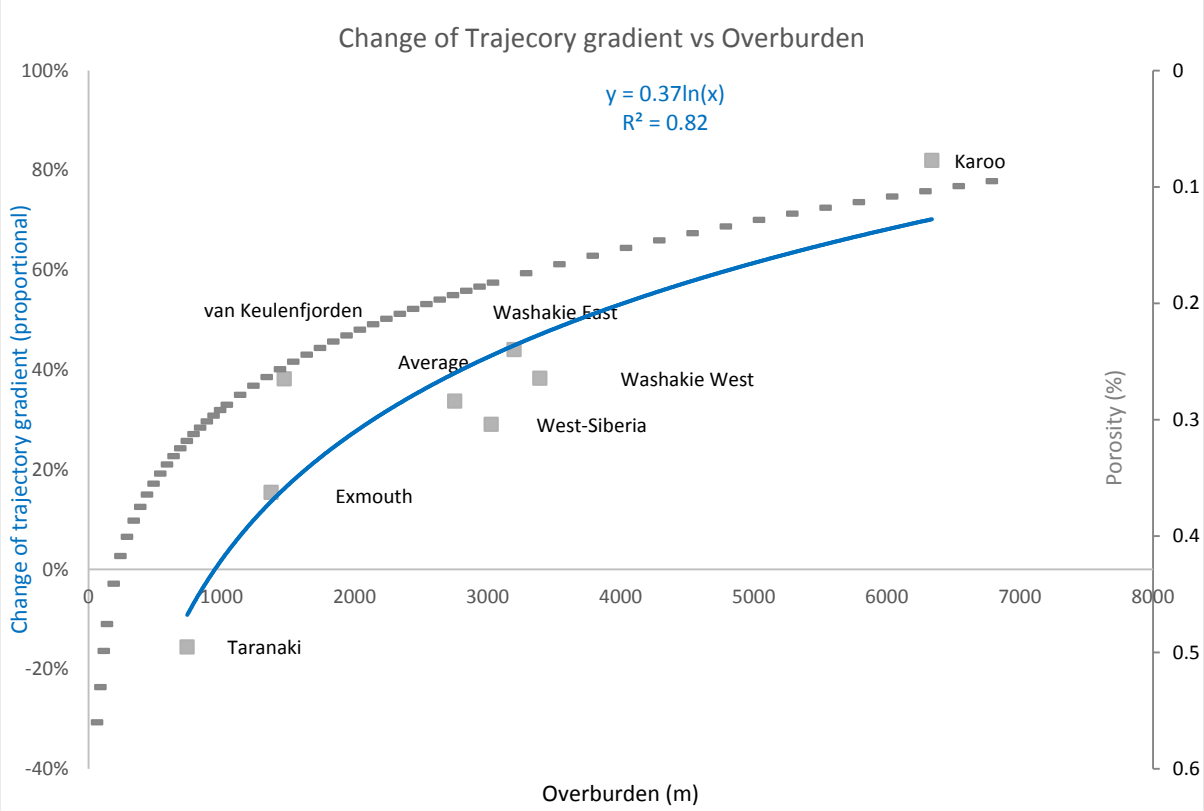

Graph 2. Logarithmic fit between extent of the overburden and exagerration of trajectory gradients. Grey curve is porosity/depth relation of a 50/50 Sand Shale mixture (Sclater and Christie, 1980). Notice similarity in trend; as volume increases, trajectory is stretched vertically, exaggerating gradients proportionally.

Implications to stratigraphy

Because of differential compaction, apparent forced regressions could have been deposited during a phase of normal regression. Thus, differential compaction distorts the apparent arrangement of the sedimentary fill as defined by stacking patterns, systems tracts and sequence stratigraphy (Van Wagoner et al., 1988). This implies that differential compaction imposes a lithologically controlled factor onto the traditional understanding of stacking patterns and sequence stratigraphy.

Indicators such as topset aggradation can be used to complement geometric interpretations as these can signpost aggrading trajectories regardless of their present-day orientation.

Furthermore, as systems tracts and stacking pattern architectures are associated with a particular suite of hydrocarbon plays differential compaction impacts petroleum play analyses (Catuneanu et al., 2009; White, 1980). Consequently, the novel sequential decompaction methods outlined in this study could benefit exploration.

Potentially erroneous interpretations can be avoided by examining pattern stacking in a lithological context to supplement geometric observations. In summary, it is suggested to be cautious when making stratigraphic interpretations when there is limited lithological control in the form of core or well data.

Implications to deepwater sediment bypass

Trajectory gradients and orientations are genetically and statistically linked to the extensiveness of deepwater sand in the deeper regions of the basin (Dixon et al., 2012; Gong et al., 2015a).

Orientations of slightly falling and straight trajectories are rotated upwards during sequential compaction. Subsequently, they are exaggerated further in non-sequential compaction (figure 19). Both effects act to make apparent, present-day geometries seem more prone to coarse grained sediment bypass than their reconstructed, syn-depositional counterparts. Thus, falling-to-rising adjustments in conjunction with the observed exaggeration of mainly rising trajectory gradients could result in overly optimistic predictions of deepwater sand extensiveness. This indicates that observers should be conservative in their predictions of the extensiveness of deepwater sands in undecompacted data. In case considerable basinward fining is present, upward trajectory reorientations should be anticipated. When this is the case, predictions of deepwater sand extensiveness should be conservative because apparently falling trajectories may be the result of distortion. A quantitative disquisition of alterations in statistical links due to geometry and trajectory distortion is presented in Part 2 of this study.

	Scale dependant	**Lithology dependant**	**During deposition of succession**	**After deposition of succession**	**Effect on slope gradients and clinoform heights**
Non-differential compaction	No	No	Yes	Yes	Decrease
Differential compaction	No	Yes	Yes	No	Increase
Isostatic subsidence	Yes	No	Yes	Yes	No

Table 5. Factors distorting syn-depositional clinoform geometries and trajectories after burial.

Distortion of clinoform morphologies

Sequential compaction alters clinoform geometries, defining parameters for these geometries such as slope lengths and topset/foreset ratios are modified accordingly. In addition, sequential decompaction experiments reveal deformation of strata underlying prograding shelf-edges. Commonly, reconstructed geometries have a more bottom-heavy divergent morphology with a less sigmoidal overall shape, including a low-gradient slope.

Though clinoformal sequences within a succession appear consistent in their dominantly sigmoidal shape, the primary, syn-depositional geometry was notably different as they undergo alterations of defining characteristics due to differential compaction. Several of these geometries are used to infer processes surrounding the shelf and deepwater. Notably, slope gradients and slope lengths, which are associated with triggering and placement mechanisms of turbidites and MTCs (Hampton et al., 1996).

Further research on the effect of compaction on shelf-edge and slope systems will benefit the understanding of such distortions.

The effectiveness of reconstructing clinoform geometries with sequential decompaction

To assess the effectiveness of our new decompaction method, we compare the geometry of a reconstructed clinoform to that of an unburied, lateral equivalent in the same formation (Giant

Foresets Formation, Taranaki Basin, offshore New Zealand, figure 20). Morphological similarities and similarities in measured clinoform height and slope gradient are observed between the unburied and reconstructed clinoforms. This supports the effectiveness of our new method. The results also show that a large component of observed falling trajectory.

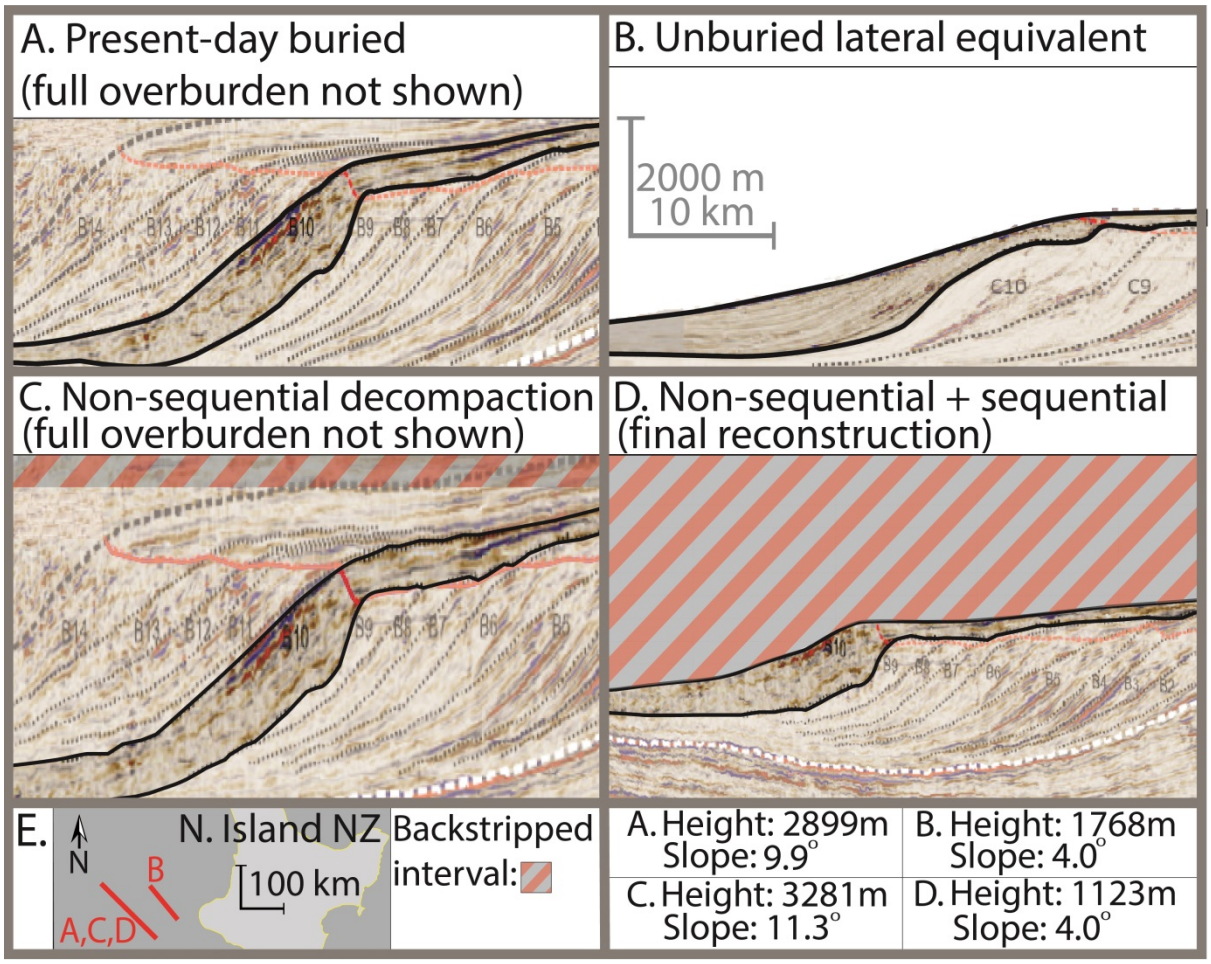

Figure 20. Comparison between syn-depositional and buried geometries of laterally equivalent clinoform in Taranaki Basin. Note the high accuracy in geometry between present-day and reconstructed equivalent.

Clinoform bulges

Downward bulging of strata below the centre of the clinoform could be caused by differential loading. Because most the vertical column of sediment is highest around the inflection point of the strata, this is where the greatest amount of compaction occurs.

Clinoform bulges are a common feature in sequentially decompacted clinoform geometries (appendix 4). Thus, it is believed to be a common, short-lived feature in unburied clinoforms. Following further succession development, the feature is healed as loading becomes uniform along-dip of the clinoform due to further progradation of the shelf-edge. Clinoform bulges could potentially effect lateral migration of hydrocarbons and source rock maturation (Coleman 2017, personal communication; Lenhart 2017, personal communication).

Isostatic subsidence

The weight of sequence-scale clinoforms applies a significant isostatic depression on underlying strata and earth's crust during succession development (Steckler et al., 1999). Thus, there is a

transient downward displacement of the shelf-edge with respect to eustatic sea level. This generates auto-accommodation, permitting aggradation irrespective of changes in eustasy. Consequently, apparently rising shelf-edge successions are recorded in the stratigraphy even during episodes of eustatic sea-level fall or quiescence (figure 21).
This effect is only relevant on large (shelf-edge) scale since smaller systems and model experiments are not massive and long-lived enough to overcome crustal rigidity and create a substantial isostatic subsidence. Therefore, this effect should be accounted for in physical models that simulate basinal responses to eustatic signals (Thijs 2017, personal communication).
This study does not account for the time-dependent component of isostasy. Considering the timescale of shelf-edge clinothem deposition (ca. 102–104 ka according to Patruno et al., 2015b), subsidence is expected to approach isostatic equilibrium. Further experiments that implement more complex lithologies and time-dependencies are likely to achieve even more accurate reconstructions of unburied shelf-edge trajectories and clinothem geometries although the overall dynamics and effects of differential compaction and isostasy will remain the same.

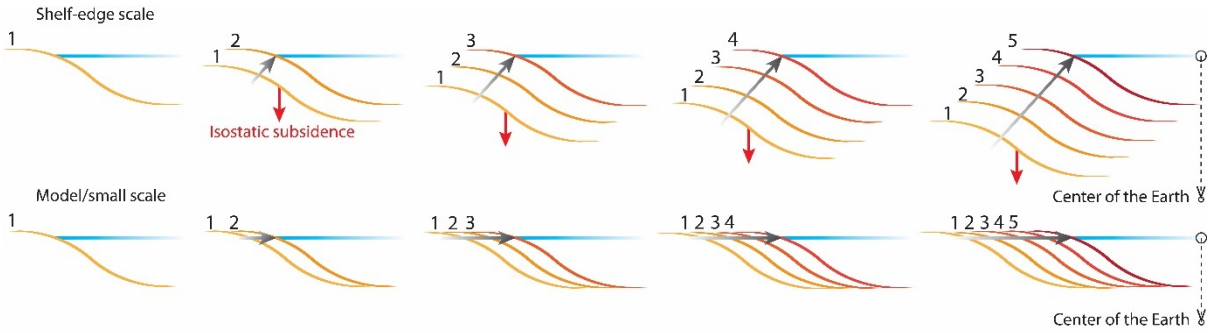

Figure 21. Effect of isostatic subsidence in large-scale shelf-edge system compared to a small-scale system.

Restoring paleo-horizontal orientation of reefs

Reef organisms thrive in a roughly consistent depth below the sea surface to maintain a preferential equilibrium position between sufficient sunlight and submersion (Darwin, 1897). For this reason, platforms reefs are constructed approximately parallel to the surface of the sea. Following burial, sequential compaction alters the horizontal paleo-orientation of reef platforms (Koša et al., 2015). Accurate reconstruction of the orientation of syn-depositional clinoformal strata containing reefs can therefore be judged by means of determining the deviation from horizontal in the reef platform. Figure 15 shows the differences between reef platform tilts; deviations from the horizontal before and after sequential decompaction. The results show that following sequential decompaction, reef tilt is decreased substantially. It can be argued that reconstruction of more horizontal orientation in the tilt of platform reefs is an indicator that sequential decompaction is effective for reconstructing syn-depositional clinoform geometries. It should be noted that there are very large uncertainties associated with the decompaction of carbonates.

Orbitally controlled RSL in Washakie Basin?

A study of local biostratigraphy in the Washakie Basin suggests that the 16 sequences represented by Lewis-Fox Hills clinoformal succession were deposited in approximately 1.5 Ma (Carvajal and Steel, 2009). Thus, the average time of deposition for one sequence is approximately 100 Ka. Since every sequence represents one cycle of RSL rise and subsequent fall, a 100 Ka periodicity in RSL

suggests that the basin could have been subjected to orbital eccentricity controlled sea level fluctuations during deposition. If this were true, additional eccentricity cycles such as the 400 ka and 2.3 Ma periods should be superimposed on the 100 Ka signal.
Evidence for these additional cycles is found following the reconstruction of RSL fluctuations by means of sequential decompaction (figure 18). Sequential decompaction transforms the basinward trend in clinoform height to an apparently cyclic pattern. A discrete Fourier transform indicates that the period of cyclicity revealed by sequential decompaction has a period of approximately 400 Ka (Graph 3).

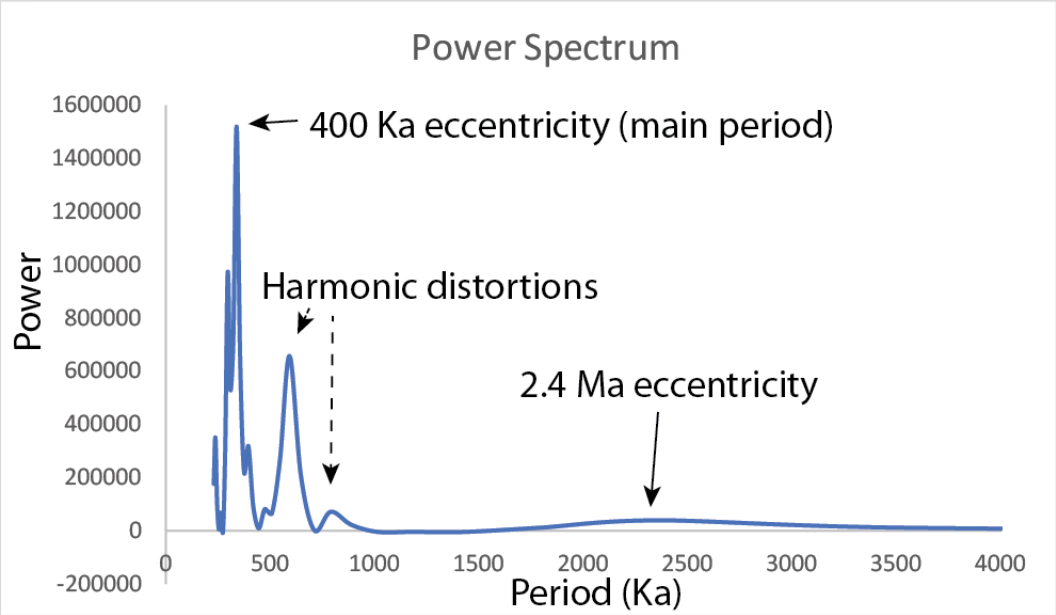

Graph 3. Power spectrum of sequentially decompacted clinoform heights (figure 18) suggesting the presence of multiple eccentricity cycles.

Additionally, a gradual increase in amplitude of the 400 Ka curve hints at a third expression. This is observation is supported by a broad peak with low amplitude in the power spectrum with an apex at 2.3 Ma. This peak however cannot be proven to be significant since entire succession represents only 1.5 Ma, not enough to display a full 2.3 Ma cycle.
These observations form tentative arguments to support the theory that the depth of Washakie Basin was regulated by orbitally controlled sea level fluctuations. This would in term indicate that sequential decompaction allows for high precision in reconstructions of RSL fluctuations, revealing trends that are not visible in unaltered or non-sequentially decompacted clinoform successions. It should be noted that the following study; (Abreu et al., 1998) argues that orbital cyclicity has been detected in a $\delta^{18}O$ signal from the Late Cretaceous greenhouse, during which the Washakie Basin succession was deposited. This indicates that during this time, high amplitude glacial/interglacial eustatic sea level variations could have been present.

CONCLUSIONS

Using a newly developed decompaction method that accounts explicitly for downdip lithological heterogeneities within clinothems, it has been demonstrated that differential compaction during the deposition of a clinoform succession has major implications on shelf-edge trajectories. This is because clinothems originally deposited during normal regression can be modified to form apparent forced regression stratigraphic architectures after burial. This alters the apparent arrangement of the sedimentary fill as defined by shelf-edge trajectory of syn-depositional stacking patterns. The approach also affects predictions of the timing of coarse-grained sediment transfer into the deep basin. Our case studies show that differential compaction during the deposition of clinoform successions can cause a net increase in slope gradients and clinoform heights by preferentially compressing foreset and bottomset strata that impact paleobathymetric estimation. This steepens the slope and vertically extends the height of the clinoform. Therefore, widely used non-sequential decompaction methodologies that do not account for lithological heterogeneities within clinothems are flawed, and may even be counter-effective in reconstructing syn-depositional clinoform heights and slope gradients, and predicting the timing of sediment transfer from the continents, across the shelf-edge, and to the ocean. Furthermore, our sequential decompaction technique shows that rising, aggradation-dominated trajectories can form irrespective of sea-level variations due to the transient application of loading subsidence caused by the deposition of shelf-edge deltas.
Accurate RSL fluctuations were reconstructed using the novel technique. In the Washakie Basin dataset, cyclicity is revealed with a set of periods that could correspond to orbital eccentricity cycles. Substantial simplifications and uncertainties are associated with the novel methodology. Therefore, further research is needed to benefit the understanding of differential compaction and its implications.

The effect of differential compaction on shelf-edge trajectories

Part II: Implications to predictive capacity

ABSTRACT

Shelf-edge trajectories and other geometric parameters of shelf-edge clinoforms successions carry predictive merit to the extensiveness of deepwater sands on the basin floor. However, differential compaction following burial substantially distorts clinoform trajectories and geometries, potentially decaying predictive capacities. Here we present a quantitative account of statistical linkages amongst a suite of geometric and lithological measurements of shelf-edge clinoform successions. We then, for the first time, quantitatively assess the effects of (differential) compaction induced geometry distortion on the decay of statistical correlations. To achieve this, we calculate rank-based correlation coefficients and significance values from measurements of two well-studied shelf-edge clinoform successions: Washakie Basin (well log correlation panel) and outcrop: van Keulenfjorden (outcrop). After applying a decompaction method that considers differential compaction, geometric parameters are measured and correlated again, allowing us to quantitatively determine the benefit of geometry reconstruction by means of decompaction by looking at the changes in the correlation coefficients.

Results indicate that trajectory gradients and topset/foreset ratios correlate significantly to sand volumes on the basin floor. Geometry reconstruction by means of decompaction substantially increases the total sum of all correlation coefficients (21% Washakie Basin, 14% van Keulenfjorden) and thus appears to benefit the predictive capacity of shelf-edge trajectory and clinoform geometry analyses significantly.

Predicative capacity of shelf-edge trajectories

There is a co-genetic link between the gradients and orientations of shelf-edge trajectories and the timing and extent of their associated deepwater sand deposits (Dixon et al., 2012; Steel and Olsen, 2002; Stevenson et al., 2015; figure 4). Previous studies have shown that the measured trajectory gradients and orientations can be linked directly to down-dip volumes of basin floor fans (figure 22, 23). For these reasons, trajectories provide sedimentologists with a predictive tool. Since basin floor fans and other deepwater sand deposits can be effective hydrocarbon reservoirs, shelf-edge trajectories can thus be used as a tool for hydrocarbon exploration.

This study aims to support co-genetic links by statistically correlating sequential trajectory gradients to the volumes of their associated basin floor fan deposits, similar to (Gong et.al. 2015a). The difference is that in this study, the extent of deepwater sand deposition is linked to trajectory gradients within the same succession (figure 23). Thus, volumes of deepwater sands are linked to the gradients of their respective trajectory increments within a shelf-edge system, rather than comparing the trajectory gradients of different systems (figure 23).

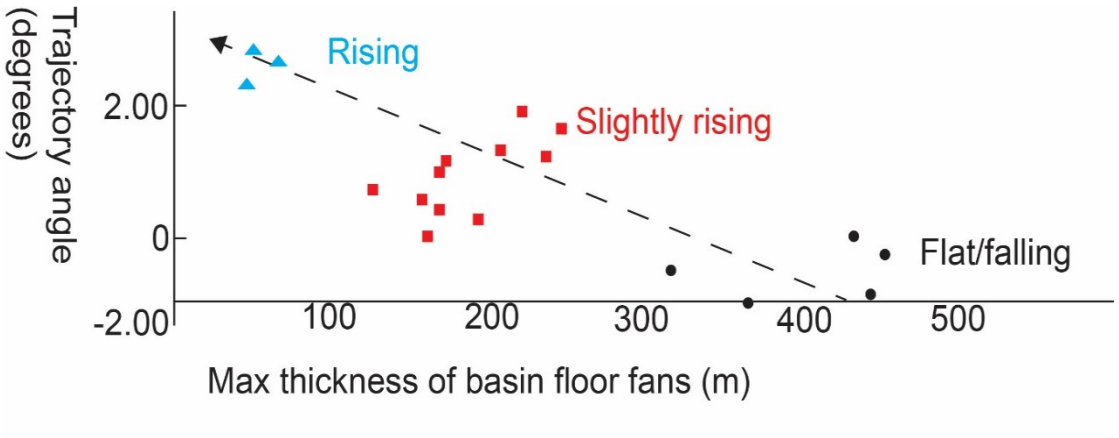

Figure 22. Adapted from (Gong et.al. 2015a). This figure illustrates the link between the thickness of down-dip sandy deposits and trajectory angle.

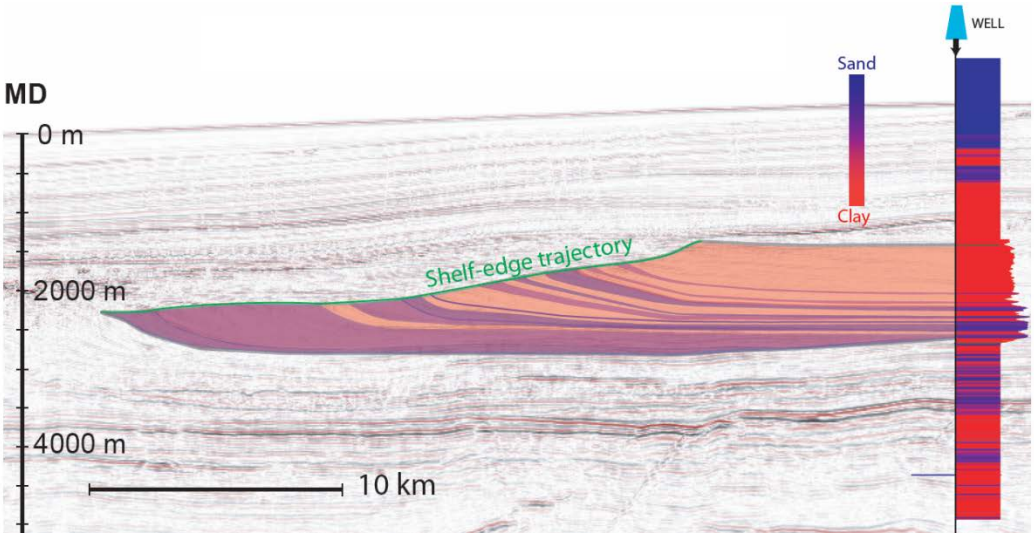

Figure 23. Shelf-edge trajectory profile from Exmouth Plateau. Sand/shale measurements derived from a gamma log down-dip of the clinoforms indicate that the gradient of the trajectory is linked to the deposition of sandy material down the shelf.

Improving correlations by reconstructing compacted geometries

During succession development, differential compaction has been shown to distort key geometric parameters of shelf-edge clinoforms, including shelf-edge trajectory gradients and orientations. These distortions of syn-depositional geometries could cause geometric proxies to be disrupted which then deteriorate statistical correlations. It is therefore hypothesized that distortion of the geometric parameters brings about a measurable decay in statistical correlations. This causes a decrease in the predictive capacities of trajectory analyses and reduces the potential of the technique with respects to hydrocarbon exploration.

The aforementioned geometric distortions caused by burial can be reconstructed by means of decompaction. If a certain distorted geometry has predictive capacity, a reconstructed geometry should have stronger predictive capacity, indicated by a stronger correlation. Geometry and trajectory distortions are substantial therefore; an improvement in statistical correlation should be measurable following decompaction.

Aims

The aim of this study is threefold: (1) Support predictive capacities of shelf-edge clinoform geometries by establishing statistical correlations. (2) Determine to what extent the distortion of clinoform geometries due to (differential) compaction affects statistical correlations. (3) Determine whether the decompaction methodologies are an effective tool for improving correlations and therefore, predictions of the extent of deepwater sand deposits.

Predictive capacity of geometric shelf-edge parameters

Aside from shelf-edge trajectories, various studies have demonstrated predictive capacities of geometric parameters related to the geometries of shelf-edge clinoforms (Anell and Midtkandal, 2015; Gong et al., 2016; Carvajal et al., 2009; Sømme et al., 2009; Patruno et al., 2015b).

In this study, a collection of these geometric parameters that has been shown to carry predictive merit is correlated to a suite of lithological target parameters such as the volume of basin floor fan systems (figure 24).

1. *Topset Surface*: The surface of the topset compartment in dip-section. When more material is sequestered in the sandy topset compartments, less sand is will be bypassed toward deeper water. Thus, there could be inverse relation between the topset surface in dip-profile and extensiveness of its associated coarse grained sediments down-dip. (Carvajal and Steel, 2009)
2. *Foreset Surface*: Large foresets indicate progradation dominated systems with low gradient trajectories and therefore, efficient bypass. Also, foreset volumes are linked to turbidity currents which could contribute to sand deposition on the slope and basin floor (Kostic et al., 2002).
3. *Bottomset Surface*: Large bottomsets consist partly of sandy material bypassed from the shelf-edge. Thus, the size of this compartment could be linked to the total amount of sandy material on the basin floor (Carvajal and Steel, 2009).
4. *Topset/Foreset ratio*: The ratio between the surface areas of the topset, foreset and bottomset in dip-section. If proportionally large amounts of sediments have been sequestered in the topset compartments, the system is likely inefficient in bypassing sediments to the basin floor. Also, this ratio is linked to the types of delta that construct the shelf (Edmonds et al., 2011). Delta types are in turn linked to the development of hydrological flows, hyperpycnal flows and deepwater fan deposition (Dixon et al., 2012).
5. *Clinoform height*: The clinoform height or amplitude corresponds to the depth of the basin (Plint et al., 2009). Basin depth could correspond to global climate which also controls erosion and precipitation, important factors for the transport of sediment from the hinterland to the basin.
6. *Slope length*: The basinward face of the clinoform in dip-section view is known as the slope length. The following study: (Sømme et al., 2009) has previously established statistically significant relationships between the slope length and the volume of basin floor fans in between shelf-systems. The rationale says that longer slopes accumulate more coarse sediment that eventually ends up on the basin floor.
7. *Trajectory height*: The height of the trajectory corresponds to the amount of aggradation (Gong et al., 2015a). This in turn infers the system's effectiveness in bypassing sediments across the shelf-edge.
8. *Trajectory gradient*: Evidence for direct statistical linkage between basin floor fan volume and trajectory gradients is demonstrated in (Gong et.al. 2012).
9. *Trajectory length*: The distance between rollover points is indicated by the sequential trajectory length. It is argued that variations in trajectory length are linked to the delta types and sediment dispersal (Edmonds et al., 2011).
10. *Slope gradient*: The gradient of the slope is linked to the stratigraphic grade as defined by (Pyles et al., 2011). This is in term connected the overall shape of the clinoform and sediment supply to the deep basin. Also, turbidity currents and submarine mass transports are controlled by this parameter (Hampton et al., 1996).

Lithological target parameters

The main lithological target parameter is sand volume on the basin floor. This is commonly deposited in the form of basin floor fans (BFFs). However, because this parameter could not be measured directly due to data limitations, lithological target parameters outlined below are instead proxies for the volume of basin floor sands.

11. Basin floor fan surface: the surface of basin floor fan depositions in dip-section are used as a proxy for the overall fan volume and thus, deepwater sand extensiveness. Obtained from (Steel and Olsen, 2002)
12. Basin floor fan thickness: Basin floor fan thicknesses are measured as a proxy for fan volume, additionally, this relates to vertical connectivity of fan bodies. Obtained from (Steel and Olsen, 2002)
13. Bottomset sand/shale ratio: A higher percentage of sand indicates more shelf-edge sediment bypass. Obtained from (Carvajal and Steel, 2012)
14. Volume of sand in the bottomset. Obtained from (Carvajal and Steel, 2012). Note; this is measure of the total volume of sand in three-dimensional bottomset compartments. Thus, it is a proxy for the volume of sand in dip-section of the measured panel.

Aside from directly linking parameters to a target constituent, it can be useful to resolve interdependencies of said parameters to expose mutually reliant elements in the system. Thus, this study also links each parameter to all other others. This way, a more complete understanding of co-genetic sedimentological and stratigraphic inputs can be developed.

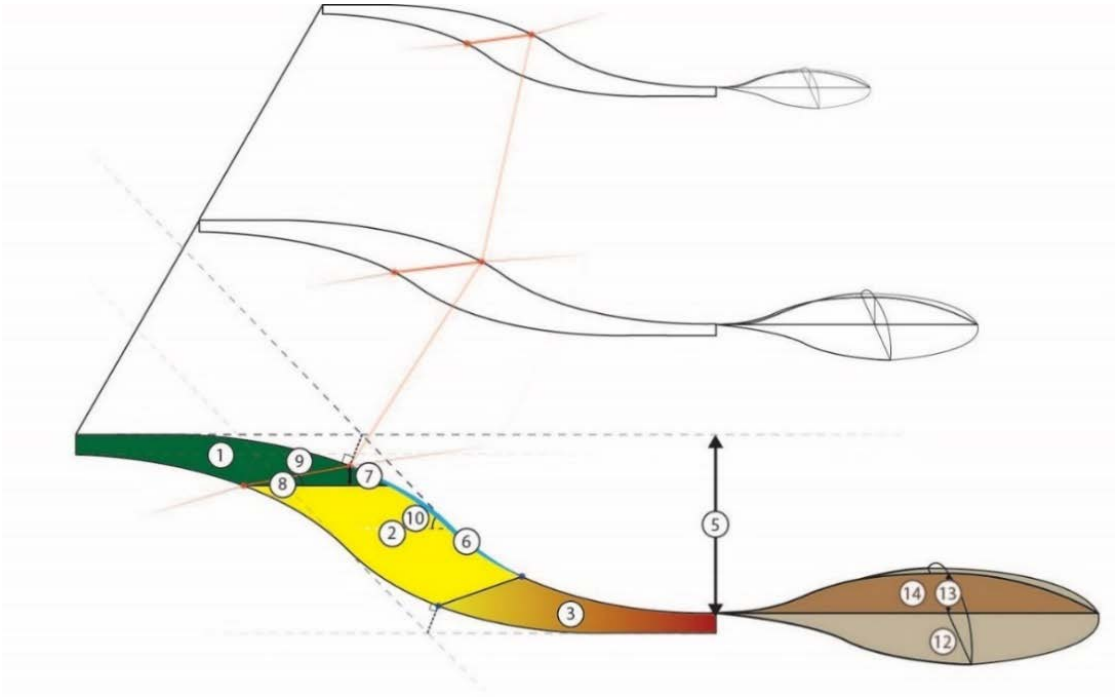

Figure 24. Parameters considered in this study.

METHODS

Decompaction and measuring methodologies

All measurements are obtained from dip-section panels of shelf-edge clinoformal systems from two datasets: (Steel and Olsen, 2002; Carvajal and Steel, 2012). The decompaction methodology outlined in Part 1 is applied. Measurements are made in the Data and Analyses module of Midland Valley's 2D Move software. Firstly, present-day geometries are measured, then these measurements are repeated following non-sequential decompaction and finally again after sequential decompaction.

Correlation and significance testing

Each parameter is measured for every clinoform sequence in the succession. Thus, every sequence is yields one data point for every parameter. A regression analyses is performed on each set of parameters. Each regression yields one correlation coefficient; a measure for the degree of correlation between two parameters. This number can be any value between 1 and -1. Where 1 is a perfect positive correlation and -1 is perfect negative correlation. 0 indicates random noise.
Because most of the inferred correlations are understudied (Gong et al., 2015b) not much is known about the trend of the relation e.g. linear or exponential. For this reason, a rank-based correlation coefficient is used. This study uses the Spearman's rank correlation coefficient: ρ, first outlined in (Spearman, 1904).
Correlation coefficients are supplemented with a significance value (P-value). This number represents the odds that a measured statistical significance of a correlation is a false positive; a result that is due to random chance rather than a genuine co-genetic relation. This number can be any value between 1 and 0 where 1 is a 100% chance of a false positive and 0 being 0% chance of a false positive. P-values are grouped in significance ranks that each represents a range of P-values. The following study; (Zar, 1972) elaborates on significance testing of Spearman's rank correlation coefficients.

Correlograms

A correlogram (sometimes called a correlation matrix) is a table in which all measured parameters are cross-correlated. It consists of a matrix of boxes that each indicates the results of one regression analysis. The PerformanceAnalytics (Carl et al., 2008) package in R software was used to construct the correlograms presented in this study.
Correlation coefficients are indicated in the top section of the correlogram. The significance ranks (P-values) are indicated by the symbols in the top right corner of each box in the correlogram: · → P≤0.05 * → P≤0.01 ** → P≤0.001 *** → =0.
The bottom section of the correlogram shows a box with a graphic depiction for each regression.

Datasets and measurements

Two datasets where considered for statistical measurements. These are the only two published datasets that indicate both the geometric and lithological makeup of shelf-edge clinoformal succession with good enough accuracy for both the construction of a reliable decompaction model and measurements for the extensiveness of deepwater sands:
1. Washakie Basin, the following study: (Carvajal and Steel, 2012) describes a high-resolution quantitative description of the Washakie-Great Divide Basin clinoformal basin fill located in Wyoming, United States. This high-resolution study was achieved by a generous dataset of 620 well-

log measurements in the area. Not only does this allow for a high-confidence decompaction model, it also be used determine the extensiveness of deepwater sand bypass within the shelf-edge succession.

The shelf-edge succession is buried bellow 3300 meters of overburden and is therefore significantly distorted due to compaction. Eleven sequence-scale clinoforms could be measured accurately. Thus, there are eleven data points for each regression from this dataset (n=11).

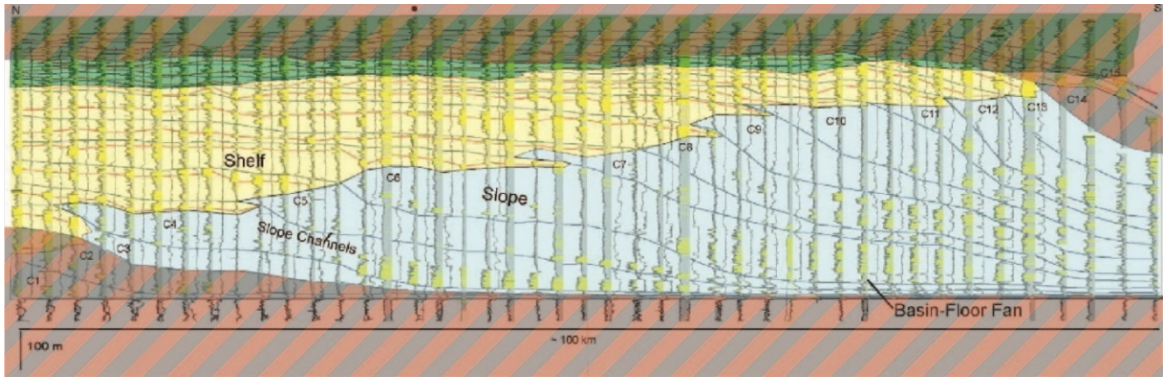

Figure 25. Western profile of the Washakie basin clinoformal succession as presented in (Carvajal and Steel, 2012). The striped overlay indicates the interval excluded used for measurements (n=11).

2. Van Keulenfjorden, a uniquely exposed clinoformal shelf-edge outcrop located on the island of Spitsbergen, Norway. Basin floor fan deposits also outcrop in this area. Their thicknesses and surfaces in section view are shown in (Steel and Olsen, 2002). Not all sequences represented in the outcrop are displayed completely on the interpretation panel. For this reason, only sequences 5 to 13 and 15 are considered for the correlations. (Sequence 14 does not fully display the extent of the basin floor fans). Thus, a total of ten sequences-scale clinoforms were measured (n=10).

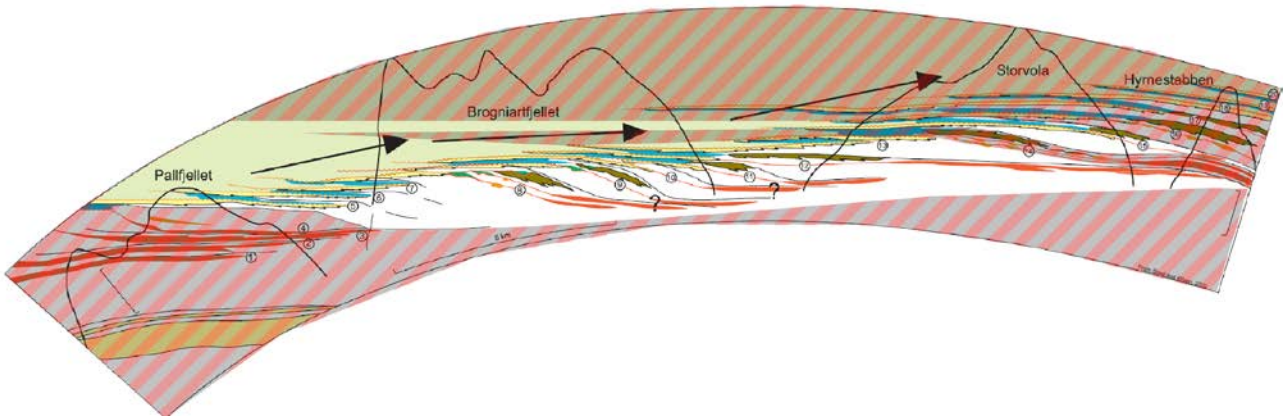

Figure 26. van Keulenfjorden outcrop as presented in (Steel and Olsen, 2002). The striped overlay indicates the interval excluded used for measurements (n=10).

Measurements

This section outlines the measurements of each geometric and lithological target parameter. Measurements are for present-day (red) and decompacted (green) geometries. Spreadsheets outlining all measurements are included in the appendix (appendix 6). A present-day geometry correlogram and a decompacted geometry correlogram of either dataset is included to show interdependencies of all parameters. Additionally, a set of smaller correlograms that only include target parameters are shown. The correlograms show a total of 336 regression analyses; 168 per dataset, 84 per correlogram.

Washakie Basin present-day	Topset Surface (km^2)	Foreset Surface (km^2)	Bottomset Surface (km^2)	T/F Ratio	Clinoform Height (m)	Slope Length (m)	Trajectory Width (m)	Trajectory Height (m)	Trajectory Gradient (°)	Trajectory Length (m)	Slope Angle (°)	Sand/Shale Bottomset (%)	Sand Volume Bottomset (km^3)
Table 6.1. Measurements for present-day clinoform trajectories and geometries of the Washakie Basin dataset													
C3	0.48	1.27	0.60	0.26	191	20945	56	56	43.36	79	0.31	0	0.1
C4	0.69	2.93	0.80	0.18	248	20199	16093	24	0.08	16093	0.34	26	49.1
C5	0.67	2.94	0.50	0.19	309	28050	5364	66	0.71	5365	0.34	13	19.7
C6	1.52	3.88	0.77	0.33	350	17651	21822	40	0.10	21822	0.53	40	65.9
C7	0.45	1.28	0.92	0.20	363	11336	6391	28	0.25	6391	0.75	23	18.8
C8	1.11	1.40	2,00	0.33	405	11952	5629	49	0.50	5629	0.70	34	39.9
C9	0.59	1.80	0.76	0.23	390	15974	3377	62	1.06	3378	0.69	38	48.2
C10	0.4	1.91	3.11	0.08	384	5764	13411	-31	-0.13	13411	1.16	55	52.6
C11	0.71	0.58	0.60	0.60	351	5440	2119	59	1.60	2120	1.87	43	15.8
C12	0.59	0.98	1.49	0.24	308	7578	5795	-7	-0.07	5795	1.32	73	45.3
C13	0.5	0,97	0.12	0.01	260	5055	2616	33	0.73	2616	1.26	30	7.1
Table 6.2 Measurements for sequentially decompacted clinoform trajectories and geometries of the Washakie Basin dataset													
C3	0.28	1.17	0.75	0.15	417	25885	56	103	54.41	117	0.00	0.1	0.1
C4	0.95	2.04	0.66	0.35	417	38058	16093	86	0.31	16093	0.26	49.1	49.1
C5	1.07	2,00	1.61	0.30	374	33614	5364	135	1.44	5366	0.13	19.7	19.7
C6	1.36	1.16	1.07	0.61	409	19306	21822	127	0.33	21822	0.40	65.9	65.9
C7	0.77	3.94	1.54	0.14	370	14011	6391	83	0.75	6392	0.23	18.8	18.8
C8	1.08	3.86	1.81	0.19	442	11954	5629	115	1.17	5630	0.34	39.9	39.9
C9	2,00	3.04	4.14	0.28	427	18110	3377	151	2.56	3381	0.38	48.2	48.2
C10	0.86	2.78	1.54	0.20	348	7456	13411	-8	-0.03	13411	0.55	52.6	52.6
C11	2.86	8.35	6.12	0.20	394	5441	2119	119	3.22	2123	0.43	15.8	15.8
C12	1.45	6.33	1.12	0.19	441	9802	5795	-24	-0.23	5795	0.73	45.3	45.3
C13	1.43	5.82	2.76	0.17	346	9688	2616	103	2.25	2618	0.30	7.1	7.1

Table 6. measurements of each parameter of the Washakie Basin dataset.

van Keulenfjorden present-day	Topset Surface (km^2)	Foreset Surface (km^2)	Bottomset Surface (km^2)	T/F Ratio	Clinoform Height (m)	Slope Length (m)	Trajectory Width (m)	Trajectory Height (m)	Trajectory Gradient (°)	Trajectory Length (m)	Slope Angle (°)	BFF Thickness (m)	BFF Surface (m^2)
Table 7.1 Measurements for present-day clinoform trajectories and geometries of the van Keulenfjorden dataset													
seq. 5	0.26	0.10	0.10	1.30	117	1223	812	48	3.41	814	3.49	0	0
seq. 6	0.17	0.16	0.04	0.85	137	2538	737	41	3.20	738	2.17	0	0
seq. 7	0.17	0.09	0.04	1.31	142	2089	605	40	3.76	606	3.23	0	0
seq. 8	0.22	0.35	0.16	0.43	192	1456	2588	54	1.20	2589	4.41	15	61286
seq. 9	0.16	0.23	0.08	0.52	143	1260	1757	19	0.62	1757	5.93	16	29977
seq. 10	0.07	0.14	0.14	0.25	99	1271	888	12	0.75	888	4.25	19	34543
seq. 11	0.10	0.17	0.08	0.40	115	1389	1908	0	0.00	1908	3.26	20	33468
seq. 12	0.17	0.21	0.37	0.29	124	1750	2173	40	1.05	2173	0.72	29	122707
seq. 13	0.29	0.24	0.70	0.31	119	3036	2456	62	1.44	2457	1.77	0	0
seq. 15	0.24	0.27	0.01	0.86	169	1743	2777	0	0.00	2777	3,00	12	11316
Table 7.2 Measurements for sequentially decompacted clinoform trajectories and geometries of the van Keulenfjorden dataset.													
seq. 5	0.44	0.17	0.15	1.38	84	1223	812	76	5.35	816	3.4	0	0
seq. 6	0.27	0.26	0.05	0.87	86	2538	737	63	4.91	740	1.48	0	0
seq. 7	0.27	0.14	0.05	1.42	157	2088	605	73	6.91	609	2.51	0	0
seq. 8	0.36	0.58	0.25	0.43	298	1454	2588	111	2.45	2591	3.32	15	61286
seq. 9	0.26	0.39	0.13	0.50	231	1258	1757	31	1.01	1757	4.99	16	29977
seq. 10	0.11	0.23	0.24	0.23	159	1270	888	50	3.22	889	3.1	19	34543
seq. 11	0.14	0.28	0.12	0.35	166	1388	1908	32	0.95	1908	2.49	20	33468
seq. 12	0.28	0.35	0.62	0.29	148	1750	2173	67	1.76	2174	0.33	29	122707
seq. 13	0.49	0.38	0.10	1.02	120	3035	2456	103	2.41	2458	1.22	0	0
seq. 15	0.42	0.46	0.02	0.88	172	1741	2777	46	0.96	2777	1.75	12	11316

Table 7. Measurements of each parameter of the van Keulenfjorden dataset.

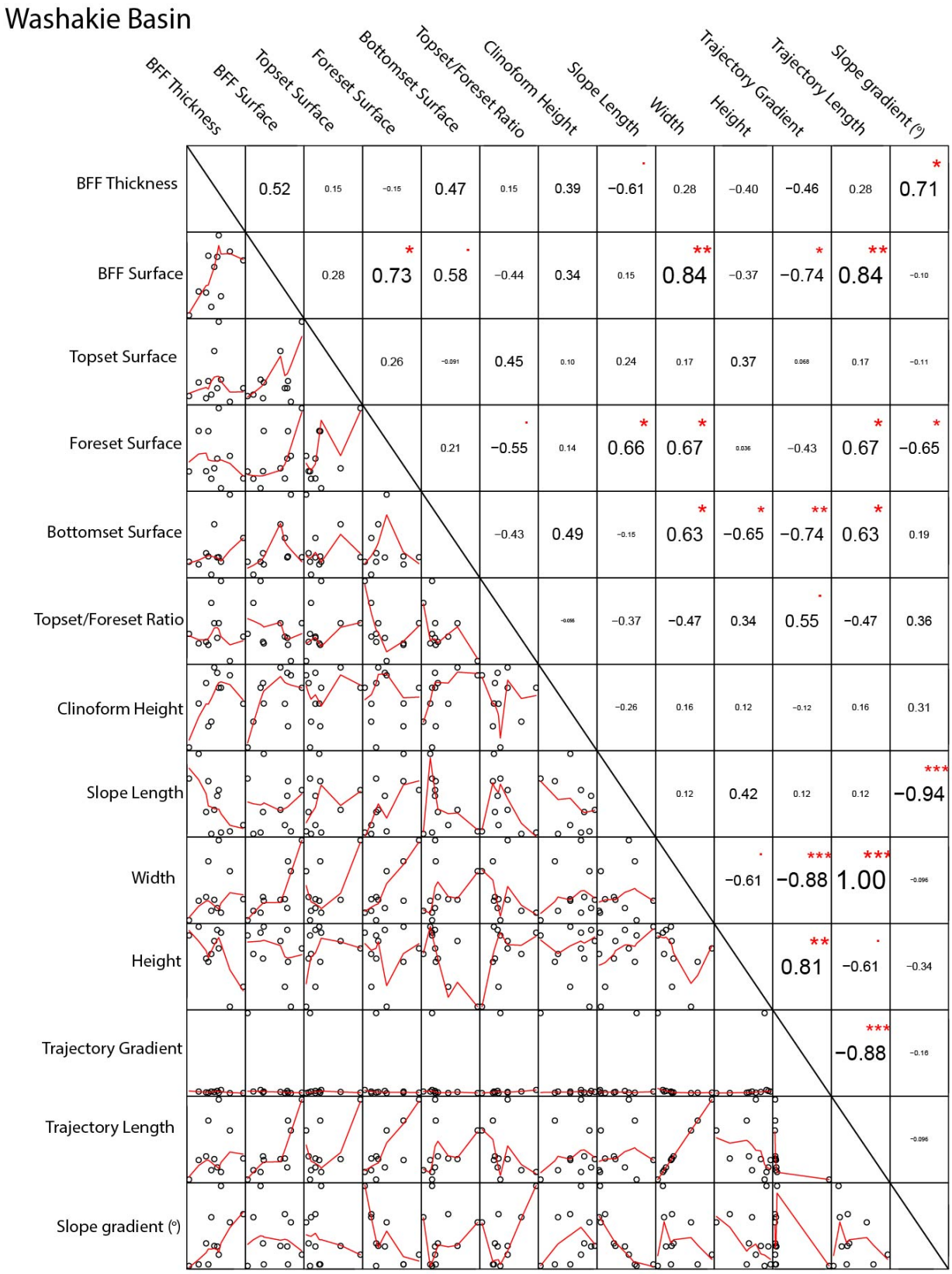

Figure 27. pre-decompacted correlogram of Washakie Basin.

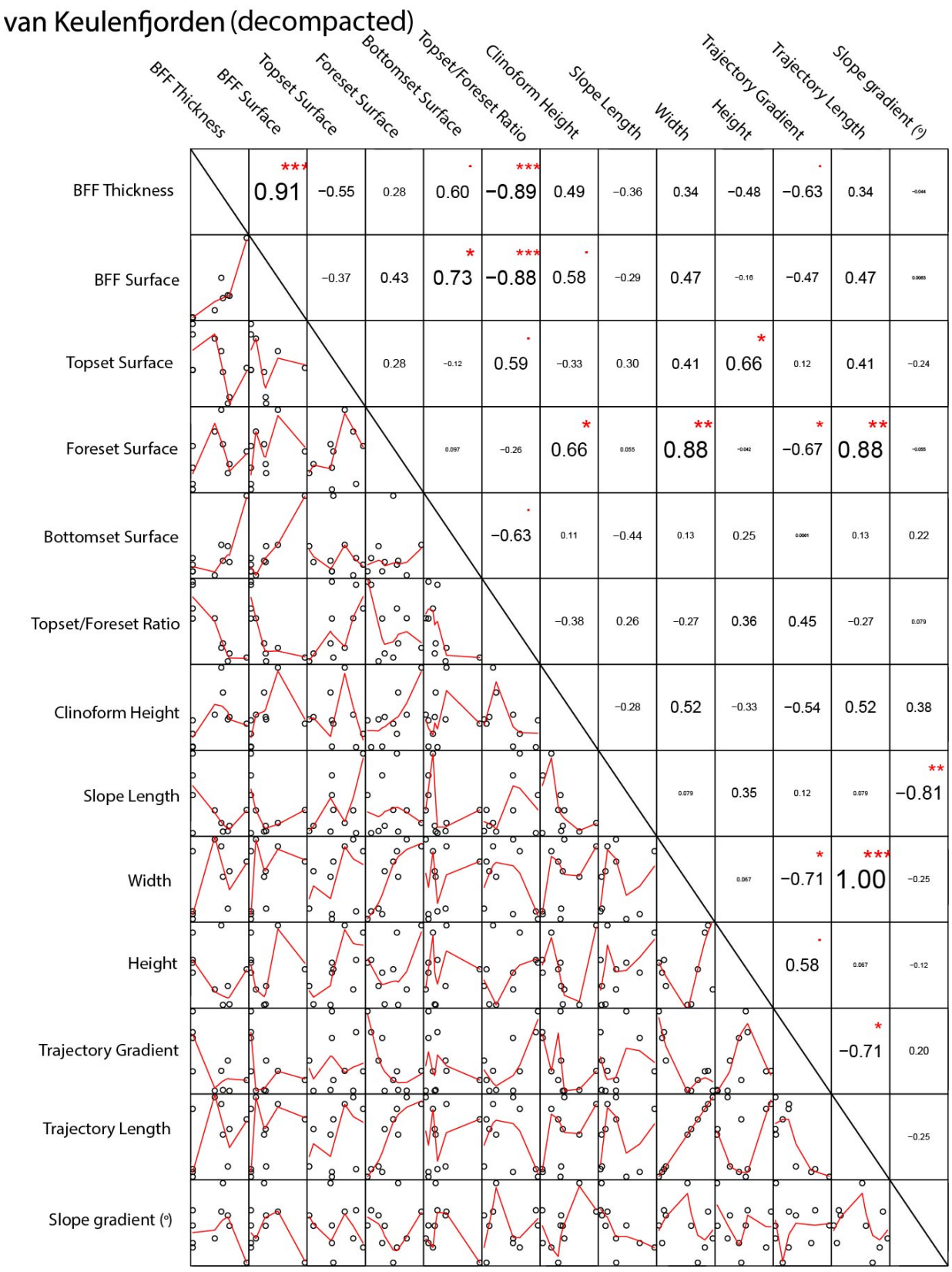

Figure 28. post-decompaction correlogram of Washakie Basin.

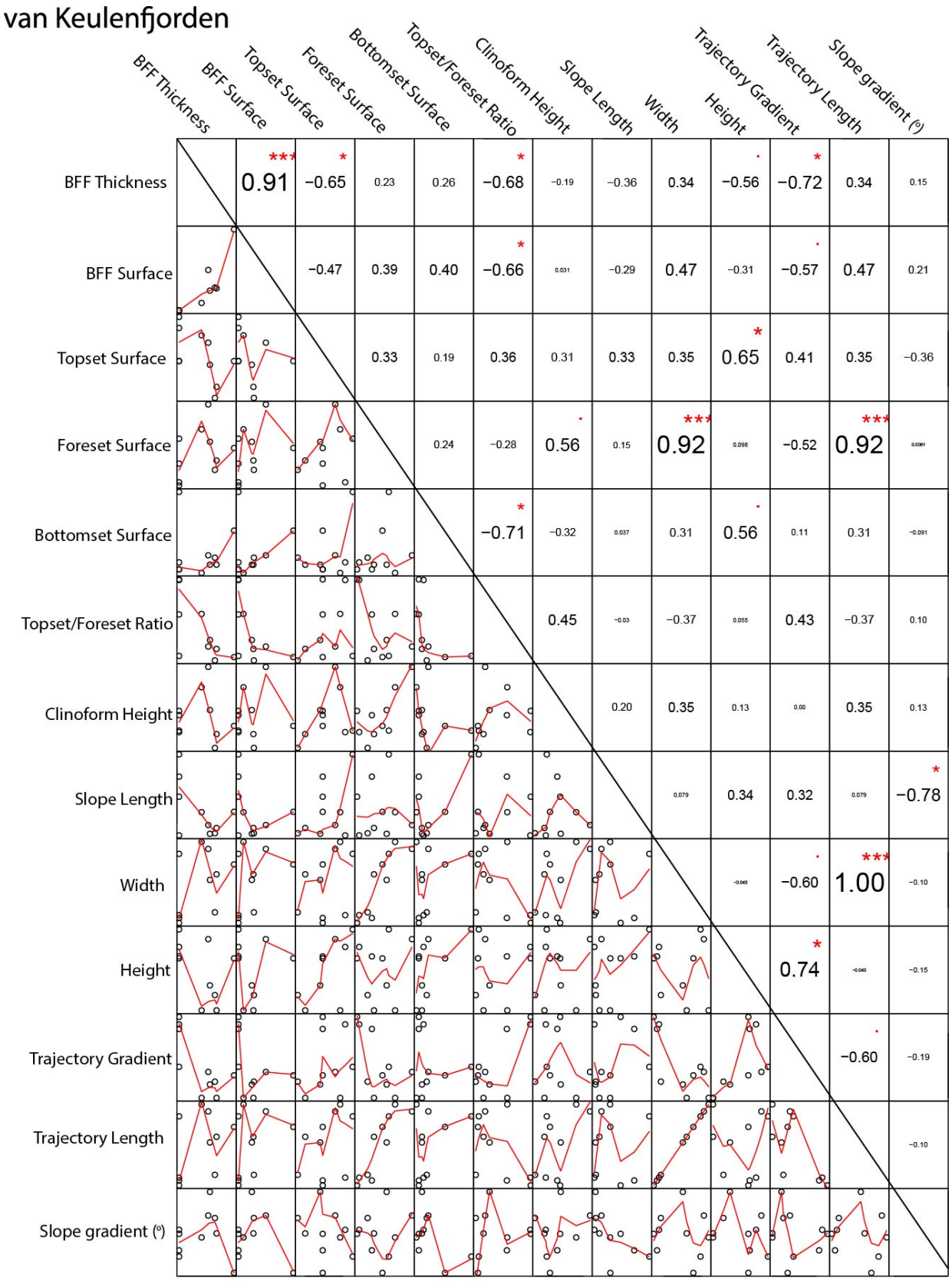

Figure 29. pre-decompaction correlogram of van Keulenfjorden.

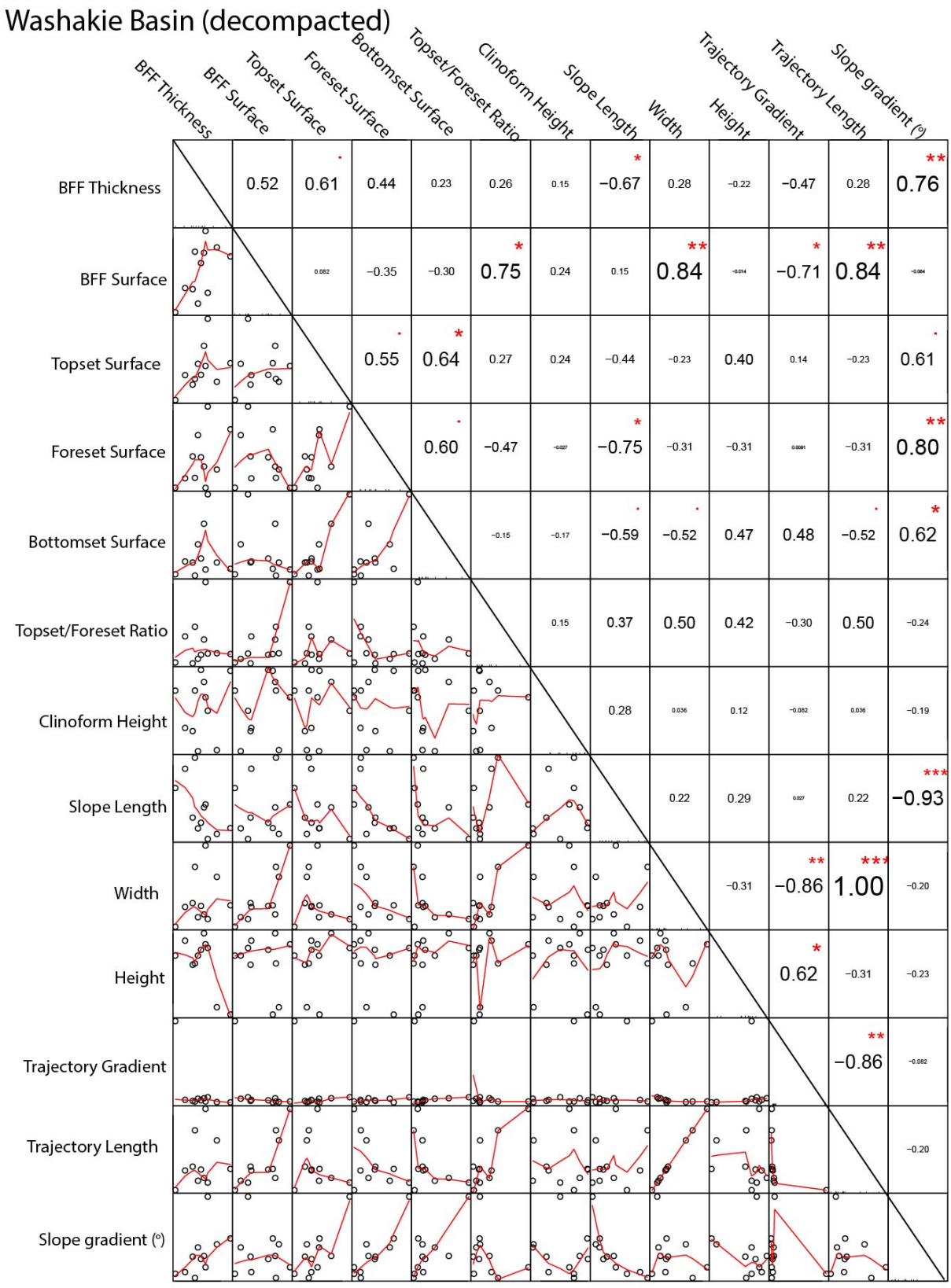

Figure 30. post-decompaction correlogram of van Keulenfjorden.

Washakie Basin sand prediction

Sand prediction correlograms for present-day (red), non-sequentially decompacted (blue) and sequentially decompacted geometries for both datasets. Both indicate a significant negative correlation between the trajectory gradient and volumes of sand. The strongest link appears to be a positive relation between sand volume and the sequential trajectory length.

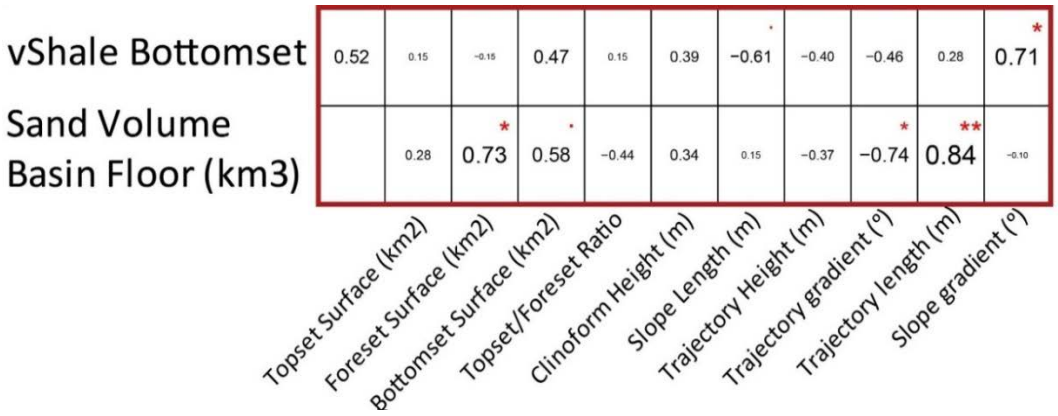

Figure 31. Sand prediction correlogram for present-day geometries. Dataset: Washakie Basin.

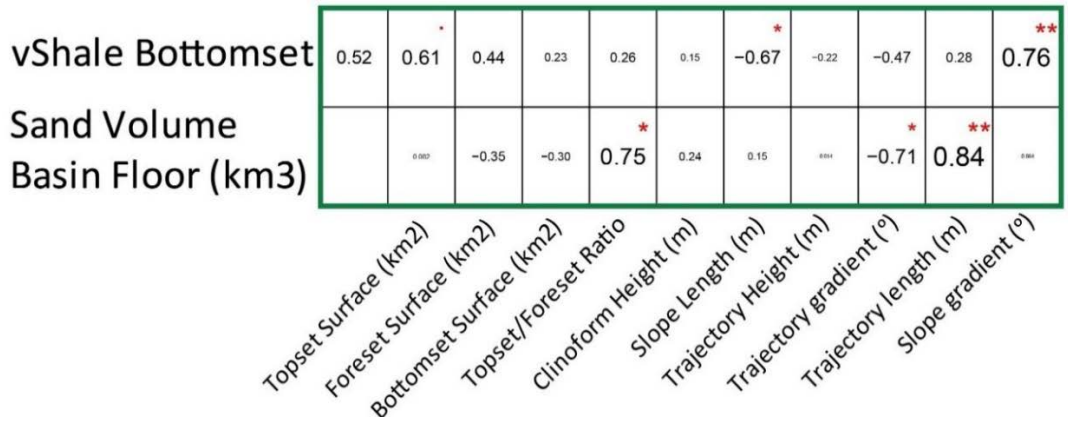

Figure 32. Sand prediction correlogram for sequentially decompacted geometries. Dataset: Washakie Basin.

Van Keulenfjorden sand prediction

There is a significant negative correlation to the trajectory gradient. The most notable correlation is a negative relation between topset/foreset ratio. This advances to an extremely significant (***) negative correlation after decompaction.

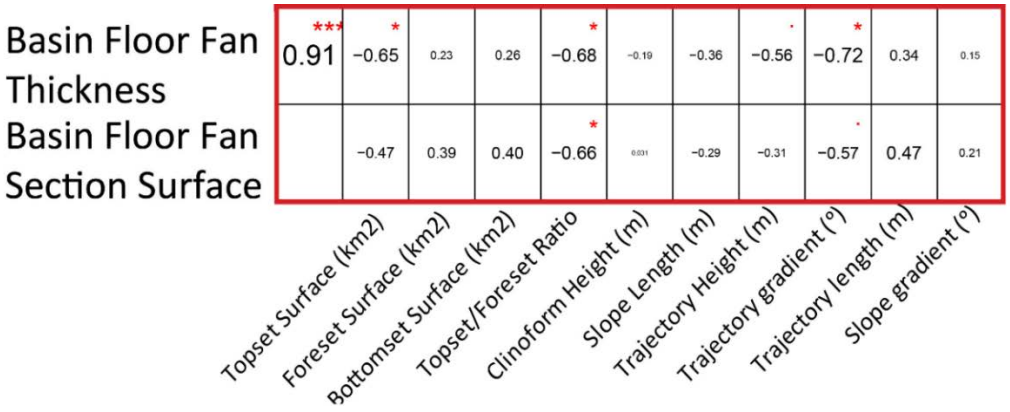

Figure 33. Sand prediction correlogram for present-day geometries. Dataset: van Keulenfjorden.

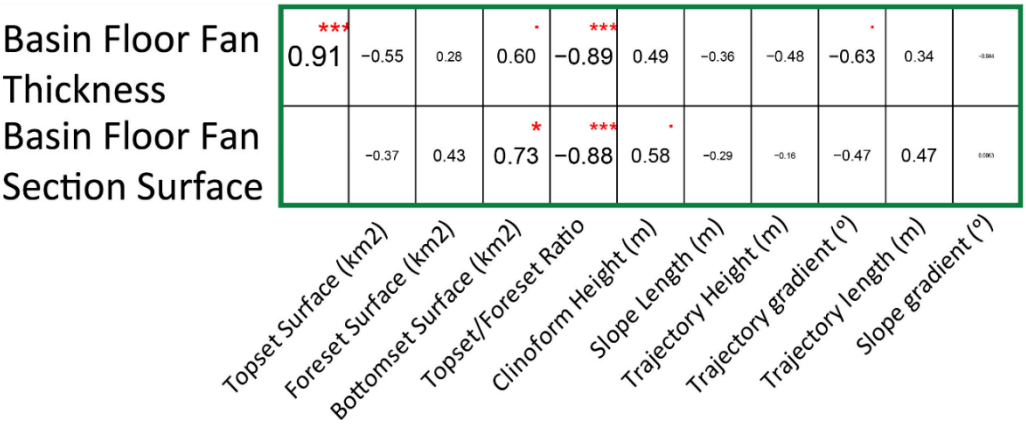

Figure 34. Sand prediction correlogram for sequentially decompacted geometries. Dataset: van Keulenfjorden.

Extent of distortion due to compaction

Several correlations improve considerably after decompaction. These include: clinoform height, trajectory gradient and T/F ratio.

To get an overall, generalised quantification for the degree of geometry reconstruction, cumulative correlation coefficients are calculated (table 8). If each undistorted parameter has a causal link to deepwater sand extensiveness, the decay in the total value for all sand correlations can be used to judge the effectiveness in geometry distortion. An increase in the cumulative correlation coefficient of sand prediction correlograms is thus an indicator for the benefit of the reconstructive capacities of the decompaction method.

There is a significant increase in cumulative correlation coefficient after both decompaction techniques (table 8). This indicates that the technique is an effective tool for improving predictions of deepwater sand extensiveness.

Cumulative correlation coefficients (sand prediction)	Pre -decompaction	Sequential decompaction
Washakie Basin	865	1066 (+23%)
van Keulenfjorden	791	904 (+14%)

Table 8. Assessing the improvements in geometry reconstructions following decompaction by means of cumulative correlation coefficients of sand prediction correlograms.

Predictive capacity of trajectory gradients

Correlation coefficients of deepwater sand extensiveness and trajectory gradients are consistently significant and illustrate a negative trend. This supports previous work: (Gong et al., 2016) where lower trajectory gradients are demonstrated to be consistent with efficient bypass. The negative relation is because lower values for trajectory gradient correlate to higher values for sand extensiveness. Decompaction does not significantly improve correlation coefficients with either dataset.

T/F ratio and trajectory length

Like trajectories, T/F ratios have strong, statistically significant negative correlations to deepwater sand extensiveness and are therefore a useful parameter for sand predictions. Low T/F ratios indicate preferential sequestration of sediment in the topsets, inferring poorly developed fluvial conduits and consequently, a small amount of sand on the basin floor. Also, there is a strong positive correlation between trajectory gradients and T/F ratios. The reason is that high-gradient trajectories indicate aggradation-dominated systems with abundant topset aggradation and coarse sediment sequestration and thus, a low T/F ratio.

A correlation between sequential trajectory length and basin floor fan volume only appears in the Washakie Basin dataset where there is a strong positive correlation. This could indicate that high overall sediment input could contribute to large amounts of basin floor sands in some settings. Also, there is a consistently strong negative correlation between trajectory gradient and sequential trajectory length. Low-angle, progradation-dominated systems appear to build out more sediment into the basin and therefore have longer trajectories.

Predictive capacity of other parameters

Topset, foreset and bottomset surface, clinoform height and slope length appear to correlate significantly in selected regressions. However, some of these parameters like topset surface, do so inconsistently; being positive in the Washakie Basin data and negative in the van keulenfjorden. In all cases, correlation coefficients for these parameters are low and significance values are low to moderate. This does not disprove any co-genetic links, but it does indicate that these links are substantially weaker than those between deepwater sand and trajectory gradients and T/F ratios. Therefore, sand predictions based on topset, foreset and bottomset surfaces, slope lengths and clinoform heights are less reliable.

One notable result is slope gradient parameter in the Washakie Basin dataset. Though this correlation changes erratically following decompaction, it does carry a strong, statistically significant positive correlation, indicating that perhaps, steeper slopes signal a higher proneness to sandy mass-transport deposits like turbidite currents or mass transport complexes. However, the same positive correlation between slope gradients and sand volumes was not found in the van Keulenfjorden data.

Randomness and uncertainty

There are three important uncertainties associated with the regression analyses performed in this study.

(1) The sample sizes are small (n=10 and n=11). This means that there is a large factor of randomness in the regression analyses.

(2) There are substantial along-strike differences in shelf-edge systems, in this study only a single dip-section panel was measured for either dataset.
(3) There are unrelated processes that occur along-strike and are thus not accounted for in measurements of dip-section panels. These processes occur parallel to processes linked to measured parameters and therefore, overprint the signal. Importantly: longshore drifts and contourites deposit substantial volumes of sand on the basin floor yet are genetically independent of localised basin floor fan deposits (Rebesco et al., 2014).
These uncertainties significantly impact the reliability of the results. However, parameters such as trajectory gradient and T/F ratio have proven to be consistently significant. Both parameters are in almost all cases within the P≤0.01 (*) significance rank. This indicates that despite randomness, uncertainties and overprinting there is a strong co-genetic relation between trajectory orientation, T/F ratios and deepwater sand extensiveness within both datasets.

CONCLUSIONS

Geometric measurements of shelf-edge clinoforms can be used to make predictions of sand volumes on the basin floor by exploiting co-genetic links. These co-genetic links can be proven and quantified by means of statistical correlation. Shelf-edge trajectory gradients in addition to T/F ratios are statistically significant geometric parameters for quantitatively predicting volumes of coarse grained sediment on the basin floor. Trajectory and geometry distortions caused by differential compaction are illustrated by a significant decay of statistical correlations. Geometry reconstructions by means of decompaction appear to significantly improve correlations in both datasets. It is therefore believed that accurate decompaction can significantly improve hydrocarbon reservoir exploration.

ACKNOWLEGDEMENTS

I would like to thank Chris Jackson, the BRG and my pod-buddies for hosting me and sharing their boundless scientific knowledge. In addition, I would like to thank David Hodgson and Dan Collins for enlightening me on clinoforms. I also thank Sian Evans, Michael Steventon, Lukas Mosser, Sharan Dhami and Jesse Zondervan because they're massive lads.
I would also like to thank Peter Burgess, Michael Blum, Ole Martinsen and Cornell Olariu for their highly constructive advice.

REFERENCES

ABREU, V. S., HARDENBOL, J., HADDAD, G. A., BAUM, G. R., DROXLER, A. W. & VAIL, P. R. 1998. Oxygen isotope synthesis: a Cretaceous ice-house?

AINSWORTH, R. B., FLINT, S. S. & HOWELL, J. A. 2008. Predicting coastal depositional style: influence of basin morphology and accommodation to sediment supply ratio within a sequence stratigraphic framework. *Recent advances in models of siliciclastic shallow-marine stratigraphy: SEPM, Special Publication,* 90**,** 237-263.

AIRY, G. B. 1856. Account of pendulum experiments undertaken in the Harton Colliery, for the purpose of determining the mean density of the earth. *Philosophical Transactions of the Royal Society of London,* 146**,** 297-355.

ANELL, I. & MIDTKANDAL, I. 2015. The quantifiable clinothem–types, shapes and geometric relationships in the Plio-Pleistocene Giant Foresets Formation, Taranaki Basin, New Zealand. *Basin Research*. 29.S1: 277-297.

BALDWIN, B. & BUTLER, C. O. 1985. Compaction curves. *AAPG bulletin,* 69**,** 622-626.

BLUM, M. D. & ROBERTS, H. H. 2009. Drowning of the Mississippi Delta due to insufficient sediment supply and global sea-level rise. *Nature Geoscience,* 2**,** 488-491.

BOWMAN, A. P. & JOHNSON, H. D. 2014. Storm-dominated shelf-edge delta successions in a high accommodation setting: The palaeo-Orinoco Delta (Mayaro Formation), Columbus Basin, South-East Trinidad. *Sedimentology,* 61**,** 792-835.

BURGESS, P. M. & PRINCE, G. D. 2015. Non-unique stratal geometries: implications for sequence stratigraphic interpretations. *Basin Research,* 27**,** 351-365.

CARL, P., PETERSON, B. G., BOUDT, K. & ZIVOT, E. 2008. PerformanceAnalytics: Econometric tools for performance and risk analysis. *R package version 0.9,* 7.

CARVAJAL, C. & STEEL, R. 2009. Shelf-edge architecture and bypass of sand to deep water: influence of shelf-edge processes, sea level, and sediment supply. *Journal of Sedimentary Research,* 79**,** 652-672.

CARVAJAL, C. & STEEL, R. 2012. Source-to-sink sediment volumes within a tectono-stratigraphic model for a Laramide shelf-to-deepwater basin: methods and results. *Tectonics of Sedimentary Basins: Recent Advances,* 131-151.

CARVAJAL, C., STEEL, R. & PETTER, A. 2009. Sediment supply: the main driver of shelf-margin growth. *Earth-Science Reviews,* 96**,** 221-248.

CATUNEANU, O. 2002. Sequence stratigraphy of clastic systems: concepts, merits, and pitfalls. *Journal of African Earth Sciences,* 35**,** 1-43.

CATUNEANU, O. 2006. *Principles of sequence stratigraphy*, Elsevier.

CATUNEANU, O., ABREU, V., BHATTACHARYA, J., BLUM, M., DALRYMPLE, R., ERIKSSON, P., FIELDING, C. R., FISHER, W., GALLOWAY, W. & GIBLING, M. 2009. Towards the standardization of sequence stratigraphy. *Earth-Science Reviews,* 92**,** 1-33.

CHEN, S., STEEL, R. J., DIXON, J. F. & OSMAN, A. 2014. Facies and architecture of a tide-dominated segment of the Late Pliocene Orinoco Delta (Morne L'Enfer Formation) SW Trinidad. *Marine and Petroleum Geology,* 57**,** 208-232.

CULLEN, A. B. 2010. Transverse segmentation of the Baram-Balabac Basin, NW Borneo: refining the model of Borneo's tectonic evolution. *Petroleum Geoscience,* 16**,** 3-29.

DARWIN, C. 1897. *The structure and distribution of coral reefs*, D. Appleton and company.

DEIBERT, J., BENDA, T., LØSETH, T., SCHELLPEPER, M. & STEEL, R. 2003. Eocene clinoform growth in front of a storm-wave-dominated shelf, Central Basin, Spitsbergen: no significant sand delivery to deepwater areas. *Journal of Sedimentary Research,* 73**,** 546-558.

DIXON, J., STEEL, R. & OLARIU, C. 2012. Shelf-edge delta regime as a predictor of deepwater deposition. *Journal of Sedimentary Research,* 82**,** 681-687.

EDMONDS, D. A., SHAW, J. B. & MOHRIG, D. 2011. Topset-dominated deltas: A new model for river delta stratigraphy. *Geology,* 39**,** 1175-1178.

FINN, T. M. & JOHNSON, R. C. 2005. Subsurface stratigraphic cross sections of Cretaceous and lower Tertiary rocks in the Southwestern Wyoming Province, Wyoming, Colorado, and Utah. *Petroleum Systems and Geologic Assessment of Oil and Gas in the Southwestern Wyoming Province, Wyoming, Colorado, and Utah: US Geological Survey, Digital Data Series, DDS-69-D*.

FLINT, S., AND, HODGSON, D., SPRAGUE, A., BRUNT, R., VAN DER MERWE, W., FIGUEIREDO, J., PRÉLAT, A., BOX, D., DI CELMA, C. & KAVANAGH, J. 2011. Depositional architecture and sequence stratigraphy of the Karoo basin floor to shelf edge succession, Laingsburg depocentre, South Africa. *Marine and Petroleum Geology,* 28**,** 658-674.

GALLOWAY, W. E. 1989. Genetic stratigraphic sequences in basin analysis I: architecture and genesis of flooding-surface bounded depositional units. *AAPG bulletin,* 73**,** 125-142.

GONG, C., STEEL, R. J., WANG, Y., LIN, C. & OLARIU, C. 2016. Grain size and transport regime at shelf edge as fundamental controls on delivery of shelf-edge sands to deepwater. *Earth-Science Reviews,* 157**,** 32-60.

GONG, C., WANG, Y., PYLES, D. R., STEEL, R. J., XU, S., XU, Q. & LI, D. 2015a. Shelf-edge trajectories and stratal stacking patterns: Their sequence-stratigraphic significance and relation to styles of deepwater sedimentation and amount of deepwater sandstone. *AAPG Bulletin,* 99**,** 1211-1243.

GONG, C., WANG, Y., STEEL, R. J., OLARIU, C., XU, Q., LIU, X. & ZHAO, Q. 2015b. Growth styles of shelf-margin clinoforms: prediction of sand-and sediment-budget partitioning into and across the shelf. *Journal of Sedimentary Research,* 85**,** 209-229.

GRUNDVÅG, S. A., HELLAND-HANSEN, W., JOHANNESSEN, E. P., OLSEN, A. H. & STENE, S. A. 2014. The depositional architecture and facies variability of shelf deltas in the Eocene Battfjellet Formation, Nathorst Land, Spitsbergen. *Sedimentology,* 61**,** 2172-2204.

HAMILTON, E. L. 1976. Variations of density and porosity with depth in deep-sea sediments. *Journal of Sedimentary Research,* 46.

HAMPTON, M. A., LEE, H. J. & LOCAT, J. 1996. Submarine landslides. *Reviews of geophysics,* 34**,** 33-59.

HANSEN, R. J. & KAMP, P. J. 2002. Evolution of the Giant Foresets Formation, northern Taranaki Basin, New Zealand.

HANTSCHEL, T. & KAUERAUF, A. I. 2009. *Fundamentals of basin and petroleum systems modeling*, Springer Science & Business Media.

HELLAND-HANSEN, W. & GJELBERG, J. G. 1994. Conceptual basis and variability in sequence stratigraphy: a different perspective. *Sedimentary Geology,* 92**,** 31-52.

HELLAND-HANSEN, W. & MARTINSEN, O. J. 1996. Shoreline trajectories and sequences: description of variable depositional-dip scenarios. *Journal of Sedimentary Research,* 66.

HENRIKSEN, S., HELLAND-HANSEN, W. & BULLIMORE, S. 2011. Relationships between shelf-edge trajectories and sediment dispersal along depositional dip and strike: a different approach to sequence stratigraphy. *Basin Research,* 23**,** 3-21.

HOLT, W. & STERN, T. 1994. Subduction, platform subsidence, and foreland thrust loading: The late Tertiary development of Taranaki Basin, New Zealand. *Tectonics,* 13**,** 1068-1092.

HUNT, D. & TUCKER, M. E. 1995. Stranded parasequences and the forced regressive wedge systems tract: deposition during base-level fall—reply. *Sedimentary Geology,* 95**,** 147-160.

JOHANNESSEN, E. P. STEEL, R. J. 2005. Shelf-margin clinoforms and prediction of deepwater sands. *Basin Research*, 17.4: 521-550.

JOHANNESSEN, E. P., HENNINGSEN, T., BAKKE, N. E., JOHANSEN, T. A., RUUD, B. O., RISTE, P., ELVEBAKK, H., JOCHMANN, M., ELVEBAKK, G. & WOLDENGEN, M. S. 2011. Palaeogene clinoform succession on Svalbard expressed in outcrops, seismic data, logs and cores. *First Break,* 29**,** 35-44.

JOHANSEN, S., GRANBERG, E., MELLERE, D., ARNTSEN, B. & OLSEN, T. 2007. Decoupling of seismic reflectors and stratigraphic timelines: A modeling study of Tertiary strata from Svalbard. *Geophysics,* 72**,** SM273-SM280.

JONES, G. E., HODGSON, D. M. & FLINT, S. S. 2015. Lateral variability in clinoform trajectory, process regime, and sediment dispersal patterns beyond the shelf-edge rollover in exhumed basin margin-scale clinothems. *Basin Research,* 27**,** 657-680.

KOO, W. M., OLARIU, C., STEEL, R. J., OLARIU, M. I., CARVAJAL, C. R. & KIM, W. 2016. Coupling Between Shelf-Edge Architecture and Submarine-Fan Growth Style In A Supply-Dominated Margin. *Journal of Sedimentary Research,* 86**,** 613-628.

KOŠA, E., WARRLICH, G. M. & LOFTUS, G. 2015. Wings, mushrooms, and Christmas trees: The carbonate seismic geomorphology of Central Luconia, Miocene–present, offshore Sarawak, northwest Borneo. *AAPG Bulletin,* 99**,** 2043-2075.

KOSTIC, S., PARKER, G. & MARR, J. G. 2002. Role of turbidity currents in setting the foreset slope of clinoforms prograding into standing fresh water. *Journal of Sedimentary Research,* 72**,** 353-362.

LANDVIK, J. Y., BONDEVIK, S., ELVERHØI, A., FJELDSKAAR, W., MANGERUD, J., SALVIGSEN, O., SIEGERT, M. J., SVENDSEN, J.-I. & VORREN, T. O. 1998. The last glacial maximum of Svalbard and the Barents Sea area: ice sheet extent and configuration. *Quaternary Science Reviews,* 17**,** 43-75.

LEMÉE, C. & GUÉGUEN, Y. 1996. Modeling of porosity loss during compaction and cementation of sandstones. *Geology,* 24**,** 875-878.

LINOL, B. & DE WIT, M. 2016. *Origin and evolution of the Cape Mountains and Karoo Basin*, Springer.

MASSON, D., HARBITZ, C., WYNN, R., PEDERSEN, G. & LØVHOLT, F. 2006. Submarine landslides: processes, triggers and hazard prediction. *Philosophical Transactions of the Royal Society of London A: Mathematical, Physical and Engineering Sciences,* 364**,** 2009-2039.

MUTO, T. & STEEL, R. J. 1997. Principles of regression and transgression: the nature of the interplay between accommodation and sediment supply: perspectives. *Journal of Sedimentary Research,* 67.

NØTTVEDT, A., LIVBJERG, F., MIDBØE, P. & RASMUSSEN, E. 1992. Hydrocarbon potential of the central Spitsbergen basin. *Arctic Geology and Petroleum Potential. Norwegian Petroleum Society (NPF), Special Publication,* 2**,** 333-362.

OLARIU, M. I., CARVAJAL, C. R., OLARIU, C. & STEEL, R. J. 2012. Deltaic process and architectural evolution during cross-shelf transits, Maastrichtian Fox Hills Formation, Washakie Basin, Wyoming. *AAPG bulletin,* 96**,** 1931-1956.

POTTER, P. E.; MAYNARD, J. B.; DEPETRIS. 2005. Pedro J. *Mud and mudstones: Introduction and overview*. Springer Science & Business Media.

PATRUNO, S., HAMPSON, G. J. & JACKSON, C. A. 2015a. Quantitative characterisation of deltaic and subaqueous clinoforms. *Earth-Science Reviews,* 142**,** 79-119.

PATRUNO, S., HAMPSON, G. J., JACKSON, C. A. L. & DREYER, T. 2015b. Clinoform geometry, geomorphology, facies character and stratigraphic architecture of a sand-rich subaqueous delta: Jurassic Sognefjord Formation, offshore Norway. *Sedimentology,* 62**,** 350-388.

PENG, Y., STEEL, R., OLARIU, C., CLAYTON, C. A. & LI, S. 2017. Transition From Storm Wave-Dominated Outer Shelf to Gullied Upper Slope: The Paleo-Orinoco Shelf Margin (Moruga Formation), South Trinidad. AAPG Annual Convention and Exhibition.

PINOUS, O., LEVCHUK, M. & SAHAGIAN, D. 2001. Regional synthesis of the productive Neocomian complex of West Siberia: Sequence stratigraphic framework. *AAPG bulletin,* 85**,** 1713-1730.

PLINK-BJÖRKLUND, P. & STEEL, R. J. 2004. Initiation of turbidity currents: outcrop evidence for Eocene hyperpycnal flow turbidites. *Sedimentary Geology,* 165**,** 29-52.

PLINT, A. G., TYAGI, A., HAY, M. J., VARBAN, B. L., ZHANG, H. & ROCA, X. 2009. Clinoforms, paleobathymetry, and mud dispersal across the Western Canada Cretaceous foreland basin:

evidence from the Cenomanian Dunvegan Formation and contiguous strata. *Journal of Sedimentary Research,* 79**,** 144-161.
PRINCE, G. D. & BURGESS, P. M. 2013. Numerical modeling of falling-stage topset aggradation: implications for distinguishing between forced and unforced regressions in the geological record. *Journal of Sedimentary Research,* 83**,** 767-781.
PYLES, D. R., SYVITSKI, J. P. & SLATT, R. M. 2011. Defining the concept of stratigraphic grade and applying it to stratal (reservoir) architecture and evolution of the slope-to-basin profile: An outcrop perspective. *Marine and Petroleum Geology,* 28**,** 675-697.
REBESCO, M., HERNÁNDEZ-MOLINA, F. J., VAN ROOIJ, D. & WÅHLIN, A. 2014. Contourites and associated sediments controlled by deepwater circulation processes: state-of-the-art and future considerations. *Marine Geology,* 352**,** 111-154.
REEVE, M. T., JACKSON, C. A. L., BELL, R. E., MAGEE, C. & BASTOW, I. D. 2016. The stratigraphic record of prebreakup geodynamics: Evidence from the Barrow Delta, offshore Northwest Australia. *Tectonics,* 35**,** 1935-1968.
REVIL, A., GRAULS, D. & BRÉVART, O. 2002. Mechanical compaction of sand/clay mixtures. *Journal of Geophysical Research: Solid Earth,* 107.
RICH, J. L. 1951. Three critical environments of deposition, and criteria for recognition of rocks deposited in each of them. *Geological Society of America Bulletin,* 62**,** 1-20.
SCLATER, J. G. & CHRISTIE, P. 1980. Continental stretching; an explanation of the post-Mid-Cretaceous subsidence of the central North Sea basin. *Journal of Geophysical Research,* 85**,** 3711-3739.
SALAZAR, M.; MOSCARDELLI, L.; WOOD, L. 2016. Utilising clinoform architecture to understand the drivers of basin margin evolution: a case study in the Taranaki Basin, New Zealand. *Basin Research*, 28.6: 840-865.
SØMME, T. O., HELLAND-HANSEN, W., MARTINSEN, O. J. & THURMOND, J. B. 2009. Relationships between morphological and sedimentological parameters in source-to-sink systems: a basis for predicting semi-quantitative characteristics in subsurface systems. *Basin Research,* 21**,** 361-387.
SPEARMAN, C. 1904. The proof and measurement of association between two things. *The American journal of psychology,* 15**,** 72-101.
STECKLER, M. S., MOUNTAIN, G. S., MILLER, K. G. & CHRISTIE-BLICK, N. 1999. Reconstruction of Tertiary progradation and clinoform development on the New Jersey passive margin by 2-D backstripping. *Marine Geology,* 154**,** 399-420.
STEEL, R. & OLSEN, T. 2002. Clinoforms, clinoform trajectories and deepwater sands. Sequence-stratigraphic models for exploration and production: Evolving methodology, emerging models and application histories: Gulf Coast Section SEPM 22nd Research Conference, Houston, Texas. 367-381.
STEVENSON, C. J., JACKSON, C. A.-L., HODGSON, D. M., HUBBARD, S. M. & EGGENHUISEN, J. T. 2015. Deepwater sediment bypass. *Journal of Sedimentary Research,* 85**,** 1058-1081.
STRAUB, K. M. & PYLES, D. R. 2012. Quantifying the hierarchical organization of compensation in submarine fans using surface statistics. *Journal of Sedimentary Research,* 82**,** 889-898.
ULMISHEK, G. F. 2003. *Petroleum geology and resources of the West Siberian Basin, Russia*, US Department of the Interior, US Geological Survey.
VAIL, P. R., MITCHUM JR, R. & THOMPSON III, S. 1977. Seismic Stratigraphy and Global Changes of Sea Level: Part 4. Global Cycles of Relative Changes of Sea Level.: Section 2. Application of Seismic Reflection Configuration to Stratigraphic Interpretation.
VAIL, P. R., & MITCHUM, JR, R. M. 1979. Global cycles of relative changes of sea level from seismic stratigraphy: resources, comparative structure, and eustatic changes in sea level.
VAN WAGONER, J., POSAMENTIER, H., MITCHUM, R., VAIL, P., SARG, J., LOUTIT, T. & HARDENBOL, J. 1988. An overview of the fundamentals of sequence stratigraphy and key definitions.

VINK, A., STEFFEN, H., REINHARDT, L. & KAUFMANN, G. 2007. Holocene relative sea-level change, isostatic subsidence and the radial viscosity structure of the mantle of northwest Europe (Belgium, the Netherlands, Germany, southern North Sea). *Quaternary Science Reviews,* 26**,** 3249-3275.

WHITE, D. A. 1980. Assessing oil and gas plays in facies-cycle wedges. *AAPG Bulletin,* 64**,** 1158-1178.

WOOD, L. J. 2000. Chronostratigraphy and tectonostratigraphy of the Columbus Basin, eastern offshore Trinidad. *AAPG bulletin,* 84**,** 1905-1928.

YOUNG, F. S. 1998. Method for general image manipulation and composition. Google Patents.

ZAR, J. H. 1972. Significance testing of the Spearman rank correlation coefficient. *Journal of the American Statistical Association,* 67**,** 578-580.